

**CHARACTERIZATION OF
DUAL PHASE STEELS BY USING
MAGNETIC BARKHAUSEN NOISE ANALYSIS**

**A THESIS SUBMITTED TO
THE GRADUATE SCHOOL OF NATURAL AND APPLIED SCIENCES
OF
MIDDLE EAST TECHNICAL UNIVERSITY**

BY

MÜCAHİT KAPLAN

**IN PARTIAL FULFILLMENT OF THE REQUIREMENTS
FOR
THE DEGREE OF MASTER OF SCIENCE
IN
METALLURGICAL AND MATERIALS ENGINEERING**

SEPTEMBER 2006

Approval of the Graduate School of Natural and Applied Sciences

Prof. Dr. Canan Özgen
Director

I certify that this thesis satisfies all the requirements as a thesis for the degree of Master of Science.

Prof. Dr. Tayfur Öztürk
Head of Department

This is to certify that we have read this thesis and that in our opinion it is fully adequate, in scope and quality, as a thesis for the degree of Master of Science.

Prof. Dr Mehmet Erdoğan
Co-Supervisor

Assoc. Prof. Dr. C. Hakan Gür
Supervisor

Examining Committee Members

Prof. Dr. Şakir Bor (METU, METE)

Assoc. Prof. Dr. C. Hakan Gür (METU, METE)

Prof. Dr. Mehmet Erdoğan (Gazi Unv., TEF)

Prof. Dr. Cevdet Kaynak (METU, METE)

Dr. İbrahim Çam (METU, Central Lab.)

I hereby declare that all information in this document has been obtained and presented in accordance with academic rules and ethical conduct. I also declare that, as required by these rules and conduct, I have fully cited and referenced all material and results that are not original to this work.

Name, Last name : Mücahit Kaplan

Signature :

ABSTRACT

CHARACTERIZATION OF DUAL PHASE STEELS BY USING MAGNETIC BARKHAUSEN NOISE ANALYSIS

Kaplan, Mücahit

M.S., Department of Metallurgical and Materials Engineering

Supervisor: Assoc. Prof. Dr. C. Hakan Gür

Co Supervisor: Prof. Dr. Mehmet Erdoğan

September 2006, 50 pages

The aim of this work is to nondestructively characterize the industrial dual phase (ferritic-martensitic) steels (DPS) by the Magnetic Barkhausen Noise (MBN) method. By quenching of AISI 8620 steel specimens having two different starting microstructures, from various intercritical annealing temperatures (ICAT) in the ferrite-austenite region, the microstructures consisting of different volume fractions of martensite and morphology have been obtained. The microstructures, strength properties and hardness values were determined by conventional metallographic and mechanical tests. The measurements of the Magnetic Barkhausen Noise (MBN) were performed by using both Rollscan and μ SCAN sensor connectors. A good correlation between the martensite volume fraction, hardness and MBN signal amplitude has been obtained. MBN emission decreased as the ICAT, therefore the volume fraction of martensite increased. Moreover, MBN emission decreased as the martensite morphology become thinner. It has been concluded that MBN method can be used for nondestructive characterization of industrial dual phase steels.

Keywords: Dual phase steel, Microstructure, Mechanical properties, Magnetic Barkhausen Noise

ÖZ

**ÇİFT FAZLI ÇELİKLERİN
MANYETİK BARKHAUSEN GÜRÜLTÜSÜ ANALİZLERİ
KULLANILARAK KARAKTERİZASYONU**

Kaplan, Mücahit

Yüksek Lisans, Metalurji ve Malzeme Mühendisliği Bölümü

**Tez Yöneticisi: Doç. Dr. C. Hakan Gür
Yardımcı Tez Yöneticisi: Prof. Dr. Mehmet Erdoğan**

Eylül 2006, 50 Sayfa

Bu çalışmanın amacı, çift fazlı (ferrit-martensit) çeliklerde iç yapının Manyetik Barkhausen Gürültüsü (MBG) metodu kullanılarak karakterizasyonudur. İki farklı başlangıç iç yapısına sahip AISI 8620 çeliğinden hazırlanan numuneler, ferrit-östenit bölgesinde çeşitli kritik tavlama sıcaklıklarına (KTS) ısıtılıp yağda soğutularak, martensit hacim oranları (MHO) ve morfolojileri farklı iç yapılar elde edilmiştir. İç yapıların, mukavemet özellikleri ve sertlik değerleri geleneksel metalografik ve mekanik testlerle tayin edilmiştir. MBG ölçümleri hem Rollscan hem de μ SCAN üniteleri kullanılarak yapılmıştır. MHO, sertlik ve MBG sinyal büyüklükleri arasında iyi bir ilişki saptanmıştır. Martensit hacim oranı KTS değerinin artmasına bağlı olarak artmış, buna bağlı olarak MBG emisyonu azalmıştır. Ayrıca, MBG emisyonu martensit morfolojisinin incelenmesiyle azalmıştır. MBG metodunun endüstriyel çift fazlı çeliklerin tahribatsız karakterizasyonunda kullanılabileceği sonucuna varılmıştır.

Anahtar Kelimeler: Çift fazlı çelik, İç yapı, Mekanik özellikler, Manyetik Barkhausen Gürültüsü

To My Son

ACKNOWLEDGEMENTS

There have been many people who helped me to reaching this far, my sincere thanks to the following people:

My supervisors, Assoc. Prof. Dr. C. Hakan Gür and Prof. Dr. Mehmet Erdoğan for there guidance, understanding and continuous support throughout the study.

Dr. İbrahim Çam, METU-Central Laboratory, for the MBN measurements

Mr. Mustafa Yılmaz for his help with the tensile measurements.

Research Assistant Kemal Davut for all his help throughout the SEM studies.

Research Assistant Volkan Kılıçlı for guidance in the heat treatments and metallographic studies

Mr. Cihan Turgay Şen, Mr. Ersin Dönmezer, Mr. Hüseyin Ercan Orhan, Mr. Kayhan Özüm and Mr. Mehmet Kayadarçın for helping me look inside.

My wonderful wife Serap Cebeci Kaplan, for your love and for always being there for me.

Finally and most importantly, to my parents, for all that I am.

TABLE OF CONTENTS

PLAGIARISM.....	iii
ABSTRACT.....	iv
ÖZ.....	v
DADICATION.....	vi
ACKNOWLEDGMENTS.....	vii
TABLE OF CONTENTS.....	viii
LIST OF TABLES.....	x
LIST OF FIGURES.....	xi
CHAPTER	
1. INTRODUCTION.....	1
2. LITERATURE SURVEY.....	9
3. EXPERIMENTAL METHODOLOGY.....	14
3.1. Material.....	14

3.2. Experimental equipment and systems used in heat treatment	14
3.3. Obtaining Initial Microstructure prior to Intercritical Annealing	16
3.4. Determining A_1 , A_3 and the Martensite Volume Fraction (MVF)	16
3.5. Metallographic Inspections	20
3.6. Mechanical Test	20
3.7. Magnetic Barkhausen Noise Measurement	21
4. RESULTS & DISCUSSION	23
4.1. General	23
4.2. Results of Microstructural Investigation and Hardness Measurements	26
4.3. Results of Tension Tests	35
4.4. Results of Rollscan Measurements	39
4.5. Results of μ SCAN Measurements	43
5. CONCLUSION	47
REFERENCES	48

LIST OF TABLES

TABLES

Table 3.1 Chemical composition of AISI 8620.....	14
Table 4.1 ICAT, MVF and Hardness values of samples.....	34
Table 4.2 Mechanical Properties of Samples.....	38

LIST OF FIGURES

FIGURES

Figure 1.1 Schematic view of the microstructure of a dual-phase steel.....	2
Figure 1.2 (a) A qualitative sketch of magnetic domains in a polycrystalline material, (b) The magnetic moments in adjoining atoms change direction continuously across the boundary between domains.....	4
Figure 1.3 A typical magnetization curve, with B, the flux density, appearing to be a continuous function of H, the magnetic field.....	6
Figure 1.4 Schematic illustration of the theoretical relation between magnetic Barkhausen noise emission and the magnetization hysteresis loop.....	6
Figure 1.5 Typical Barkhausen noise signal with the RMS envelope. BNA represents the maximum amplitude of the envelope and H _{peak} the corresponding magnetic field.....	7
Figure 1.6 Schematic magnetization curves for soft and hard magnetic materials..	8
Figure 3.1 Hereaus Annealing Furnace.....	15
Figure 3.2 Schematic view of the temperature control system for the sample.....	15
Figure 3.3 Initial microstructures prior to intercritical annealing.....	18

Figure 3.4 Summary of heat treatments.....	19
Figure 3.5 Variation of the martensite volume fraction depending on the starting microstructure (Q, QQ), and intercritical annealing temperature.....	19
Figure 3.6 Dimensions of the tension test specimen	20
Figure 3.7 μ SCAN equipment.....	22
Figure 3.8 Block diagram of μ SCAN 500 system.....	22
Figure 4.1 Micrographs showing low MVF and carbide formation	24
Figure 4.2 SEM micrograph of Q724 specimen showing carbide formation in AISI 8620 specimen	25
Figure 4.3 SEM micrographs of the as-received (AR) 8620 and quenched + tempered (QT) samples of AISI 8620.....	27
Figure 4.4 Optical micrographs of the AISI 8620 samples showing the variation in the martensite volume fraction depending on the starting microstructure (Q, QQ) and intercritical annealing temperature.....	28
Figure 4.5 SEM micrographs of the AISI 8620 samples showing the variation in the martensite volume fraction depending on the starting microstructure (Q, QQ) and intercritical annealing temperature	31
Figure 4.6 Variation of hardness values of the AISI 8620 samples depending on the starting microstructure (Q, QQ) and intercritical annealing temperature	34

Figure 4.7 Variation of yield strength of the AISI 8620 samples depending on the starting microstructure (Q, QQ) and intercritical annealing temperature	36
Figure 4.8 Variation of tensile strength of the AISI 8620 samples depending on the starting microstructure (Q, QQ) and intercritical annealing temperature	36
Figure 4.9 Variation of percent elongation of the AISI 8620 samples depending on the starting microstructure (Q, QQ) and intercritical annealing temperature	37
Figure 4.10 Variation of magnetic parameter of the AISI 8620 samples depending on the starting microstructure (Q, QQ) and intercritical annealing temperature.....	41
Figure 4.11 A sketch of magnetic domains in a martensitic microstructure	41
Figure 4.12 Correlation between magnetic parameter (MP) and hardness of the AISI 8620 samples.....	42
Figure 4.13 Correlation between magnetic parameter (MP) and martensite volume fraction (MVF) of the AISI 8620 samples.....	42
Figure 4.14 Correlation between RMS (V) and hardness (HRC) of the AISI 8620 samples.....	44
Figure 4.15 Correlation between RMS (V) and martensite volume fraction (MVF) of the AISI 8620 samples	44
Figure 4.16 Relative R.M.S Voltage as a function of Relative Magnetic Excitation of the AISI 8620 samples.....	46

CHAPTER 1

INTRODUCTION

Dual-phase steels (DPS) were introduced in the late 1970's and marked the beginning of new generation of high-strength low alloy steels (HSLA). They are characterized by

- a microstructure consisting of dispersion of 20-25% martensite or islands in a soft and ductile matrix of ferrite and
- good ductility and formability at high strength levels.

The latter quality puts DPS high on the list of materials that are being considered by the automobile industry to reduce the weight of vehicles for improved economy. DPS also exhibit smooth yielding and a high initial work hardening rate. Their strength and ductility may be controlled to favour higher strength or higher ductility by alternating the martensite content resulting from thermal or thermomechanical processing.

Some important properties of DPS are as follows: DPS displays a high and rapid initial work hardening rate. Even at low forming strain levels (2% - 3%), yield strength increases approximately 145-214 MPa. DPS have a high ultimate tensile strength (UTS). UTS range from 500 to 1200 MPa for available grades. These steels have high potential for weight reduction (up to 25% as compared to equivalent conventional HSLA steels). DPS have a higher yield to tensile ratio as compared to conventional HSLA steels (0.5-0.6). This results in a higher capacity to manage vehicle crash energy. DPS have higher fatigue strength than equivalent conventional HSLA steels. DPS meets automotive application weldability needs [1].

As a consequence of the fast depletion of the energy resources in the last decades, dual phase steels having all these advantageous properties stated above started to draw attention and yielded in a wide spread usage.

The hard martensite particles provide substantial strengthening while the ductile ferrite matrix gives good formability (Figure 1.1). To produce a dual phase microstructure, the equilibrium pearlite phase needs to be eliminated, with austenite being encouraged to form martensite by rapid cooling. The conventional method for the production of DPS is by annealing low-carbon steel within the intercritical (austenite+ferrite) temperature range for a few minutes followed by cooling at a rate fast enough to transform the austenite to martensite. The amount of austenite present during the intercritical annealing is controlled by the annealing temperature, which also controls the carbon content and hardenability of the austenite. In practice the efficiency of conversion of austenite to martensite may be less than 100%, due to epitaxial growth of ferrite into austenite during the early stages of cooling. In addition to epitaxial ferrite, pearlite, bainite, and retained austenite may also be microstructural constituents, depending upon the cooling rate. The critical cooling rates need to avoid pearlite and bainite, and at which the required amount of austenite transforms to martensite, are factors in the economic production of DPS [2].

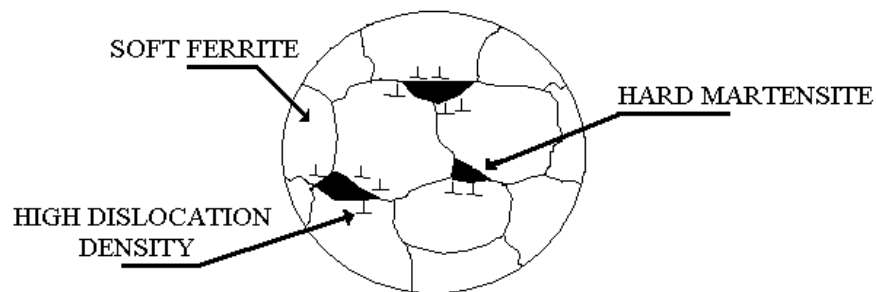


Figure 1.1 Schematic view of the microstructure of a dual-phase steel [3].

DPS are currently materials of commercial interest for the automotive industry and they have already found numerous applications including safety critical products such as side impact bars and wheel rims [4-6]. Its excellent formability and high work hardening and bake hardening behavior permit designers to reduce outer panel

gauge and weight substantially while maintaining or improving dent resistance. It offers designers the opportunity to substantially reduce closure weight, and possibly avoid substitution of more costly lower density materials. The low and intermediate tensile strength, low yield ratio grades (590 to 980 MPa TS) are frequently used in body structure applications requiring high energy absorption (i.e. the crumple zones – front and rear longitudinal rails and supporting structure). The low yield strength helps keep the initial deceleration pulse low, yet the high work hardening rate and excellent ductility absorb greater deformation energy than conventional steels. Good formability permits using these products in complicated shapes, and good weldability permits using these steels in tailored blank and hydroformed tube applications. The intermediate to highest strength grades, including the high yield ratio DP steels, are typically used in applications requiring extremely high yield strength and adequate formability, such as passenger safety cage components limited by axial buckling or transverse bending. These components (rockers, pillars, pillar reinforcements, roof rails, and cross members) rely on high yield strength to prevent intrusion into the passenger compartment during a collision. Dual phase steels enable designers to apply high yield strength steels to safety cage components that are too complex to form with the higher strength martensite steels.

Since the mechanical properties of materials depend strongly on their microstructures [7], the steel related industries spend a great deal of effort in determining and ensuring the desired microstructure. In addition, plants and structural components that have been in operation for long periods need special attention from plant operators to ensure safe and reliable performance. Efficient and economic operation of these plants requires regular preventive maintenance. It would be more effective to monitor the material condition that could lead to a subsequent failure rather than detecting a defect after its initiation. In practice, the microstructure is usually determined by optical or electron microscopy where the samples that cut from the actual product are investigated after special sample preparation. Conceivably, these methods are time consuming and a hundred percent inspection is probably impossible considering the fact that the delay in preparing the samples would affect the product's net output. Thus, there is always an interest to develop nondestructive

techniques capable of rapid evaluation. Hence, improved or new non-destructive evaluation techniques are needed to monitor microstructural changes to estimate both remaining life of the component and extent of material degradation. The magnetic Barkhausen noise (MBN) technique is one such advanced preventive maintenance tool for steel related industry [8].

Ferromagnetic materials are full of small magnetic regions called domains (Figure 1.2). Each domain is magnetized along a certain crystallographic easy direction of magnetization, and domains are separated from one another by boundaries called domain walls (Bloch walls). These domain walls move under the influence of an applied magnetic field. This movement of domain walls results in a change in magnetization within the material and will induce an electrical pulse in a pick-up coil. When the electrical pulses produced by domain movement are added, a noise-like signal (MBN) is generated, named after its discoverer Heinrich Barkhausen. Amplification of these signals produces audio/radio frequency noise, which can be observed on an oscilloscope or spectrum analyzer [8].

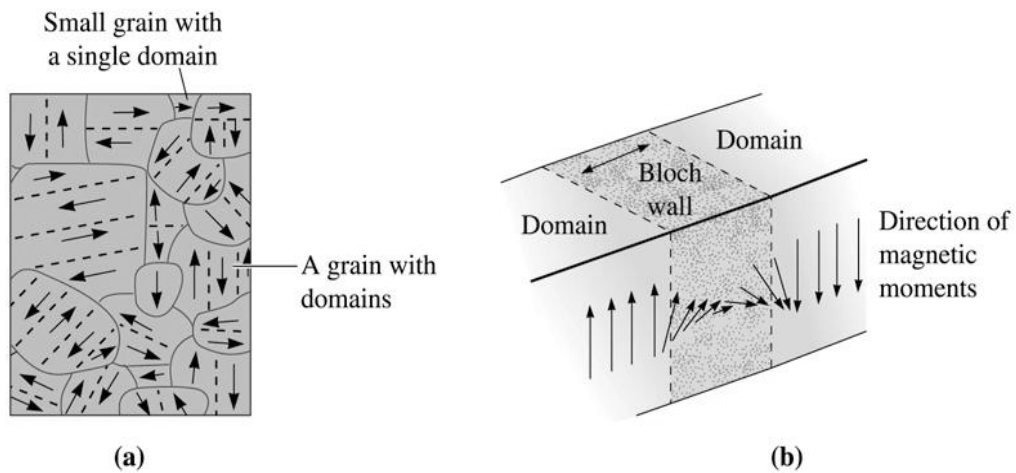


Figure 1.2 (a) A qualitative sketch of magnetic domains in a polycrystalline material, (b) The magnetic moments in adjoining atoms change direction continuously across the boundary between domains [9].

The magnetization process, which is characterized by the hysteresis curve, in fact is not continuous, but is made up of small, abrupt steps caused when the magnetic domains move under an applied magnetic field. Figures 1.3 and 1.4 show the small, discontinuous changes of B as H varies. These discontinuous changes are a result of the Barkhausen effect, i.e. small magnetization jumps due to domain walls becoming pinned and released from microstructural obstacles such as grain boundaries, second phase particles, and non-metallic inclusions. Each abrupt jump produces a brief burst of magnetic noise which can be detected and analyzed [10].

MBN has a power spectrum that extends to about 2 MHz, the amplitude of which is damped exponentially as a function of depth below the surface. The damping is attributable to eddy current damping experienced by the propagating electromagnetic fields the domain wall movement creates. Measurement depth in ferromagnetic materials depends on the frequency range of the Barkhausen emission signals and material properties, such as conductivity and permeability. The measurement range for MBN usually varies between 0.01 to 1.5 mm from the surface [8].

Two important material characteristics affect the intensity of the MBN signal. One is the presence and distribution of elastic stresses which will influence the way domains choose and lock into their easy direction of magnetization. This phenomenon of elastic properties interacting with domain structure and magnetic properties of material is called a magnetoelastic interaction. As a result of magnetoelastic interaction, in materials with positive magnetic anisotropy (iron, most steels and cobalt), compressive stresses will decrease the intensity of Barkhausen noise while tensile stresses increase it. This fact can be exploited so that by measuring the intensity of Barkhausen noise the amount of residual stress can be determined. The measurement also defines the direction of principal stresses [11].

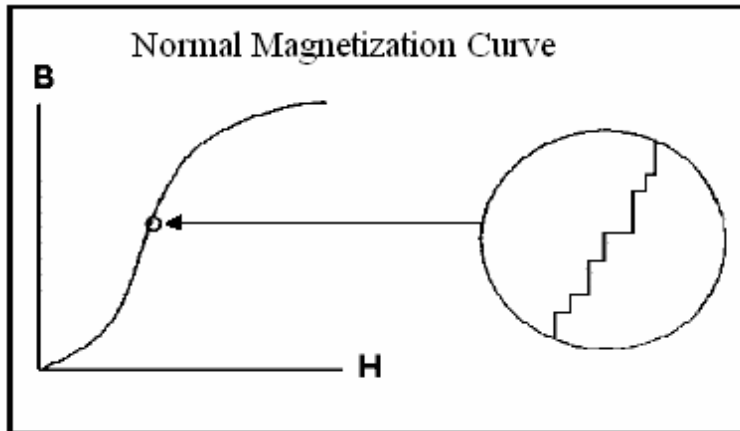


Figure 1.3 A typical magnetization curve, with B , the flux density, appearing to be a continuous function of H , the magnetic field [10].

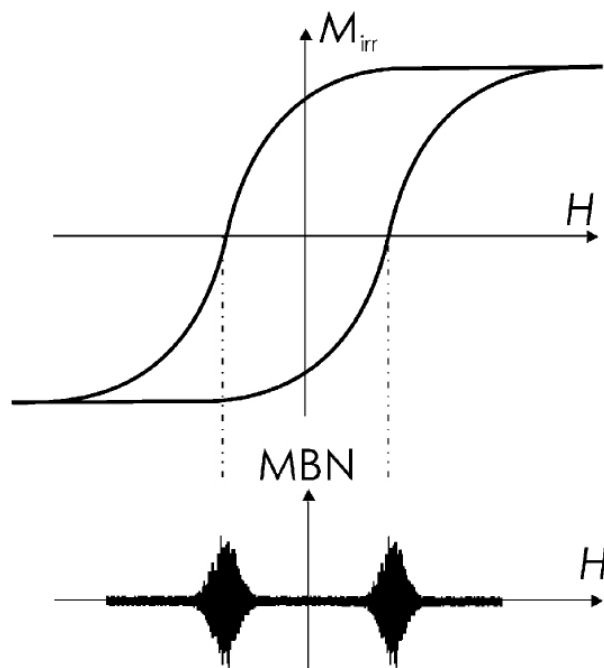


Figure 1.4 Schematic illustration of the theoretical relation between magnetic Barkhausen noise emission and the magnetization hysteresis loop [12].

It is known that magnetic parameters derived from Barkhausen emission signals that are dependent upon domain wall movement and domain nucleation, are strongly affected by the changes in the microstructure since the dimensions of the magnetic domains and the domain walls are comparable with those of phases, grains, precipitates, etc. Therefore, MBN measurements provide information on the microstructural condition of the material [11]. The MBN signal is a signature of the microstructural state of the crystal. Usually, the envelope of the signal is plotted as a function of the applied magnetic field. The envelope generally has a single-peak shape and can be characterized by different parameters (Figure 1.5), such as the maximum noise amplitude and the corresponding magnetic field. Soft magnetic materials reach their saturation magnetization with a relatively low applied field, i.e. they are easily magnetized and demagnetized. Whereas, hard magnetic materials have a high resistance to demagnetization and a large magnetic field must be applied in a direction opposite to that of the original field to reduce the magnetization of the specimen to zero after the specimen has reached its saturation magnetization (Figure 1.6). Thus, a signal peak that is close to zero relative magnetic excitation field in a MBN profile indicates that the specimen can be easily magnetized. On the other hand, the peak being far away from zero indicates that the specimen is hard to magnetize.

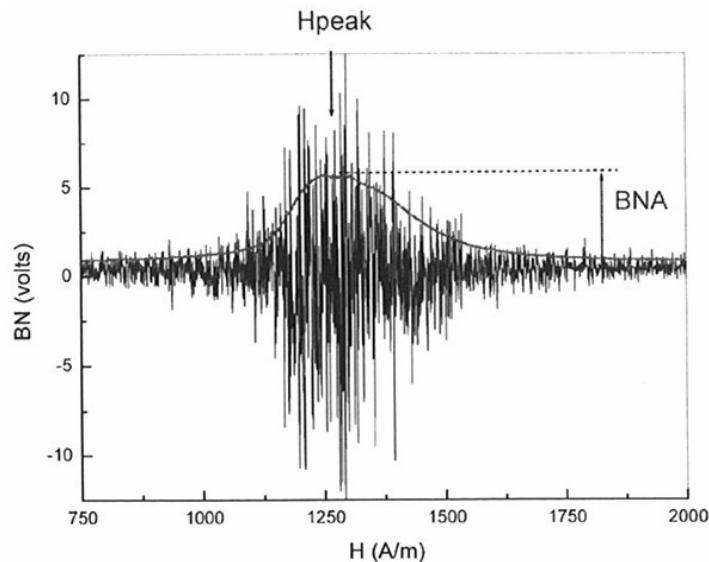


Figure 1.5 Typical Barkhausen noise signal with the RMS envelope (BNA: the maximum amplitude of the envelope, Hpeak: the corresponding magnetic field) [13].

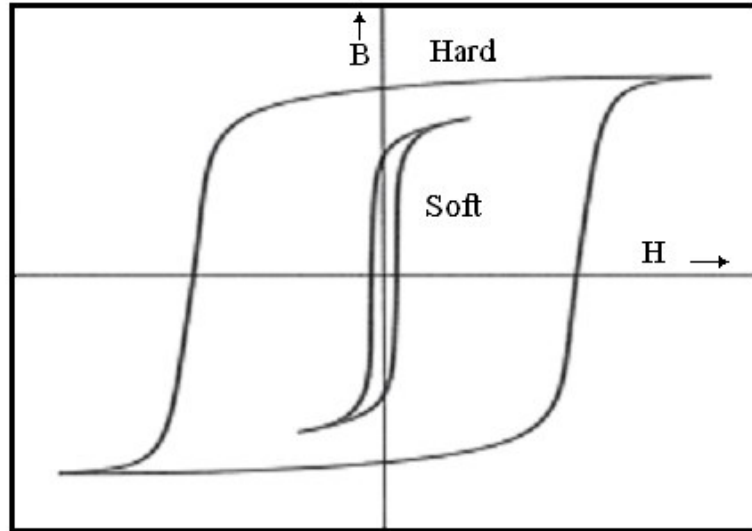


Figure 1.6 Schematic magnetization curves for soft and hard magnetic materials [14].

In this study the AISI 8620 steel samples were heated in the intercritical temperature range to obtain a microstructure consisting of austenite+ferrite, and then, quenched into oil at room temperature in order to imitate dual phase (ferrite+martensite) steel production. The aim is to investigate the possibility of characterizing the microstructure of industrial dual phase steels using Magnetic Barkhausen Noise technique.

CHAPTER 2

LITERATURE SURVEY

There are various studies showing the high sensitivity of magnetic Barkhausen noise (MBN) to changes of grain size, microstructure and stress state in the ferromagnetic materials. This chapter mainly focuses on literature survey of dual phase steels, and characterization of microstructures by MBN.

Sarwar and Priestner found that an increase in tensile strength of DPS could be obtained through an increase in martensite volume fraction as well as by an increase in the aspect ratio of martensite [15]. Tomita investigated the effect of martensite volume fraction and the morphology of the phases [16]. Bag et al. examined tensile and impact properties of high-martensite dual phase steels. They observed that equal amount of finely dispersed martensite phases exhibit the optimum combination of high strength and ductility with high impact toughness [17].

Fine dual phase structure produced more martensite than the coarse microstructure after annealing at low temperature and particular at the slower cooling rates. The reason for this was considered to result from higher carbon enrichment effect in the fine structure than the coarse ones during cooling [18].

Modi studied effects of microstructure and experimental parameters on high stress abrasive wear behaviour of a 0.19 wt % C DPS. Martensite content was noted to be significantly dependant on the heat treatment condition or the initial microstructure of the steel prior to the intercritical annealing. Marginally higher amount of pearlite and finer microconstituents are present in the normalized samples compared to that in the annealed one. In the case of the finer microstructures (finer ferrite grains and

pearlite lamellae) larger number of nucleation sites is available in the normalized samples; and this result in more nucleation sites and faster growth. Residual stress is also expected to be present in normalized steel, which further assists in higher diffusivity. Thus there is a possibility of a faster rate of ferrite to austenite transformation in the case of steel subject to normalizing then to annealing period to intercritical annealing. This may also lead to the formation of more austenite in the intercritical heating zone at a given time especially if the transformation is not complete. It is thus expected that there will be a marginally higher amount of martensite in the normalized (austenization at 890°C/1 h and air cooling) + intercritical annealing (holding at 765°C/1 h and ice-water quenching) as compared to martensite in the annealed (austenization at 890°C/1 h and furnace cooling) + intercritical annealing (holding at 765°C/1 h and ice-water quenching). The amount of austenite which transforms to martensite during quenching increases with increasing intercritical annealing temperature (ICAT). As a result the hardness and strength of steel increased with increase in martensite content. Further, it has been noted that toughness of the steel samples increase with increase in the martensite content in a dual phase ferrite-martensitic structure [19].

The metallurgical industry has been searching for methods capable of characterizing material properties accurately, quickly and easily, without damaging the material to be tested. MBN is considered as an evaluation technique of considerable importance for microstructural and mechanical characterization of steels. The advantages of this method over other methods are that it is a nondestructive economical technique, and can be easily used to evaluate samples of various shape and sizes and under different external conditions. MBN is sensitive to various parameters which effect the domain configuration and domain-wall pinning sites; these, in turn, are strongly influenced by the grain size [20,21,22] , composition [20,23], ferrite, pearlite and martensite phases [23,24], surface condition [25], hardness [26], residual stress [26,27], fatigue and damage [28], and also by the action of external factors such as the magnetic field strength [29], and applied stress [21].

The Barkhausen signal and the characteristics of the hysteresis loop (B_{\max} , dB/dH) in stressed samples are also modified by the grain size. The maximum amplitude of MBN voltage, B_{\max} and dB/dH decrease with grain size, essentially due to the fact that for fine grain samples, the number of domain and walls that can move is much bigger in these samples than in the samples with coarse grain [30]. The amplitude and shape of Barkhausen signal were correlated with the grain size in pure iron and with the presence of interstitial carbon atoms in the iron matrix in 130 p.p.m. carbon-iron alloy. The amplitude and the shape of Barkhausen signal were changed by the presence of carbon in the iron matrix. The magnetic after effect phenomenon, related to interstitial atoms, induced a decrease of the velocity and the R.M.S. voltage amplitude, and an increase of the total duration of the Barkhausen signal [21].

It is known that tempering induced the increase of MBN by increasing the mean free path of domain wall movement due to reduction in dislocation density [29]. MBN technique has been used to characterize the microstructures in quenched and tempered 0.2 % carbon steel. Tempering at 600°C showed single-peak MBN behaviour after 0.5 h and a slope change indicating the development of two-peak behaviour after 1 h. After 5h of tempering, MBN showed clear two peak behaviour. A two stage process of irreversible domain wall movement during magnetization is proposed considering the grain boundaries and second phase precipitates as the two major obstacles to domain wall movement. It has been observed that MBN generation is strongly influenced by the dissolution of martensite and precipitation of cementite particles [20]. Gür et al. concluded that MBN may provide a good opportunity for microstructure evaluation of steels and it seems to be much more sensitive to the microstructural variations in steels compared to the sound velocity measurement. Once the quantitative relationships between MBN parameters and the microstructural parameters are established, MBN method can be used efficiently and effectively for evaluating the microstructural state of the ferromagnetic steel components during fabrication or service [31, 32].

Some other studies [33, 34] showed that MBN is susceptible to the microstructures in the weld heat-affected zone. The different characteristics of the MBN signals and

magnetic relaxation was observed between martensite and bainite structures. The decrease of MBN activity and relaxation frequency due to post-weld heat treatment was attributed to the domain wall pinning due to the precipitation of carbides. The rapid increase of MBN and relaxation frequency in the intercritical region was attributed to the increase of magnetic softness associated with the change of carbide morphology. The MBN level increased with the increasing size of carbide, and the tempered bainite structure showed higher signal than the tempered martensite. The result indicated that heat-treated materials may result in microstructurally different domain wall pinning obstacles at different thermal cycles.

Kleber et al. has reported that MBN measurements could be successfully used for the characterization of ferrite-martensite steels. The temperature chosen in the intercritical region changes the volume fraction of martensite, and its carbon content. As the volume fraction of martensite increases, the MBN peak of martensite becomes narrower, greater in amplitude and shifts to a lower magnetic field. Regarding the relations found, they concluded that the measurement of the MBN signal in such steels can lead to the determination of

- martensite volume fraction deduced from the ferrite peak amplitude,
- the carbon content of the steel deduced from the martensite peak amplitude,
- the carbon content in martensite from the martensite peak amplitude as well as its field position.

These results obtained on ferrite-martensite steels have to be extended to DP steels with lower martensite volume fraction, in order to show the feasibility of using such techniques for a non destructive characterization of industrial DP steels [13].

Okazaki et al. has studied detectability of stress-induced martensite phase in ferro-magnetic shape memory alloy by MBN and concluded that MBN caused by coarse grain boundaries appear in low frequency range (1-3 kHz) in the spectrum and MBN by fine martensite twin in the higher frequency range (8-10 kHz). The envelope of the MBN voltage as a function of time of magnetization showed a peak due to grain boundaries at weak magnetic field. The MBN envelope due to martensite twins creates additional two peaks at intermediate magnetic field [35].

Blaow et al. has studied the effect of microstructure and bending deformation on the characteristics of MBN profiles in carbon steels. Microstructures associated with magnetic softness produced the largest profile peaks and the lowest peak position. Multi-peak profiles were observed in compression in spheroidized cementite specimens and to a much smaller extent in the martensite tempered at 400°C. In the spheroidized cementite, the change from a sharp single peak to a broad, three-peak profile, with a greatly reduced height was precipitous and occurred over a small strain increment. Where single peak profiles were obtained strain affected emission but did not alter the ranking imposed by microstructure. The most magnetically soft microstructure (spheroidal cementite) seems to confer little scope for a positive increase in emission with increasing strain. The most magnetically hard (martensite) showed the greatest relative strain sensitivity. All the profiles observed were reversible with respect to loading and unloading in the elastic region. The onset of plasticity did not induce any discontinuous change in the profiles whilst under load but it did induce irreversibility on unloading, due, in part, to the residual stresses induced by the inhomogeneous deformation in bending [12].

Blaow et al. studied effect of hardness and composition gradient on Barkhausen emission in case hardened steels. The shape and position of the MBN profiles significantly affected when a gradient in microstructure is induced by gradient in carbon content. On the other hand, gradient in microstructure induced by the heat treatment with a constant carbon level has much less affect on the MBN profile for the induction hardened steel [36].

CHAPTER 3

EXPERIMENTAL METHODOLOGY

3.1 Material

Carbon content was the main concern in the selection of the material. At low annealing temperatures the carbon content determines the amount of carbide formation and this third phase adversely effects the Barkhausen measurements. AISI 8620 steel (Table 3.1) was used in the experimental studies. Samples of 13.2 mm diameter and 80 mm in length were cut from a 6 m-long rod by a CNC machine.

Table 3.1 Chemical composition of AISI 8620

AISI 8620	C%	Mn%	Si%	Cr%	Ni%	Mo%	P%	S%
	0.197	0.85	0.17	0.60	0.56	0.23	-	-

3.2 Experimental equipment and systems used in heat treatment

The Hereaus annealing furnace (0-1350°C) having a sensitivity of $\pm 1^\circ\text{C}$ without atmospheric control was used in the annealing process (Figure 3.1). K-type thermocouple was used for temperature measurements. System established for temperature control is shown schematically in the Figure 3.2. The thermocouples were spot-welded at the longitudinal center of the sample. Samples were then mounted on and fixed with wires to the sample holder. Thermocouple wires were left long enough in order to keep the cold junction as far as possible from the furnace. The effect of the heat differences on the sample was minimized by placing the sample perpendicular to horizontal midline of the furnace. During the annealing process a pre-selected zone inside the furnace was used for every sample. The temperature of the sample was checked continuously on the temperature display and

any alteration in the annealing temperature was balanced by displacing the sample incrementally from the high temperature zone to a low temperature zone or vice-versa. By doing this the temperature was kept within $\pm 2^\circ\text{C}$ interval.



Figure 3.1 Hereaus Annealing Furnace

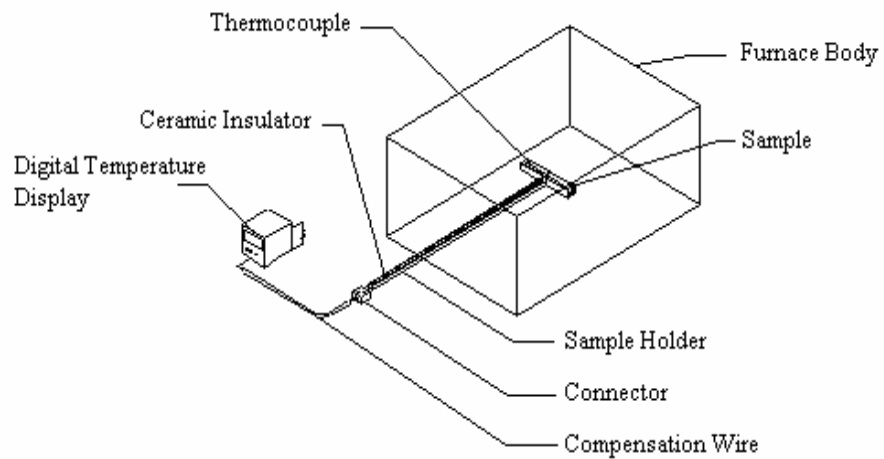


Figure 3.2 Schematic view of the temperature control system for the sample

3.3 Obtaining Initial Microstructures prior to Intercritical Annealing

A number of AISI 8620 samples having an initial pearlite + ferrite microstructure (Figure 3.3.a) were held at the intercritical temperature for 20 minutes allowing austenite to nucleate and grow at the ferrite-cementite interface. The samples were then oil quenched at ambient temperature to obtain a coarse grain martensitic microstructure in ferrite matrix. These samples are assigned as Q series (Fig. 3.4). An additional number of AISI 8620 samples were first heated to 900°C, kept at that temperature for 20 minutes allowing full austenitization and then oil quenched at ambient temperature resulting in a fully martensitic microstructure. These samples having initial microstructure of full martensite (Figure 3.3.b) were then held at the intercritical temperature for 20 minutes allowing austenite to nucleate and grow at prior austenite grain boundaries, subsequent growth occurred along many but not all of the interfaces between martensite laths. The samples were then oil quenched at ambient temperature to obtain a fine grain martensitic microstructure in ferrite matrix. These samples are assigned as QQ series (Fig. 3.4).

Due to the differences in heat absorption capacities between samples of different initial microstructures, to equalize the time period needed to reach the preset annealing temperatures, furnace temperature was increased with 4 °C for QQ series samples.

3.4 Determining A_1 , A_3 and the Martensite Volume Fraction (MVF)

The preliminary investigation was to determine the dependence of martensite volume fraction on ICAT. Andrews's formulae [37] were used to calculate the temperature values of A_1 and A_3 .

$$A_1 = 723 - 20,7xMn - 6,9xNi + 29,1xSi + 16,9xCr + 290xAs + 6,38xW$$
$$A_3 = 910 - 203xC^{1/2} - 15,2xNi + 44,7xSi + 104xV + 31,5xMo + 13,1xW$$

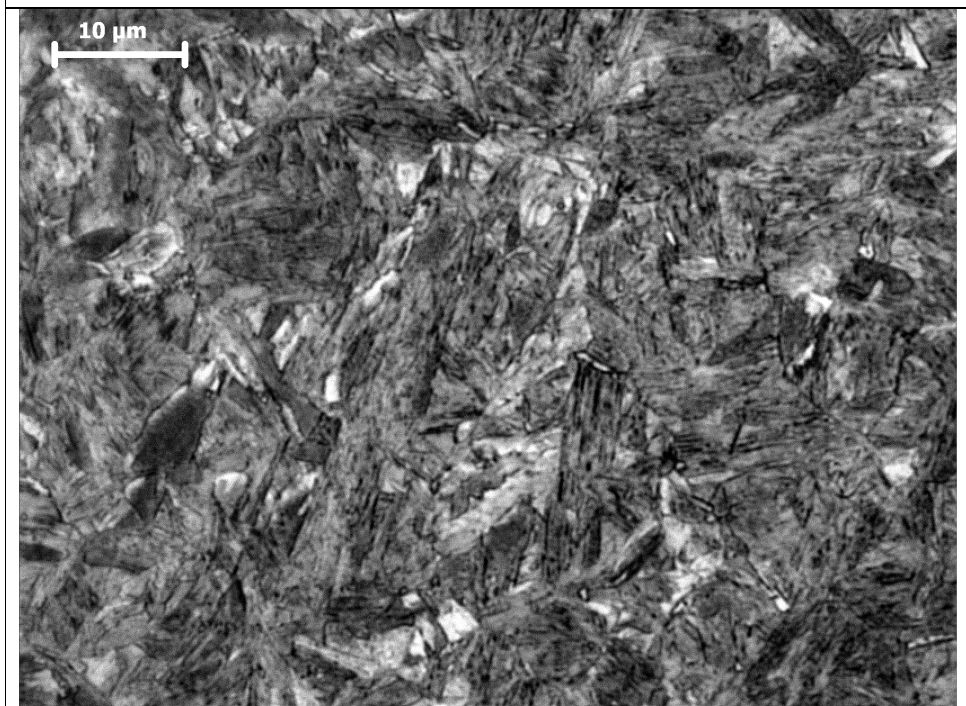
A_1 was calculated as 716°C, and A_3 as 896°C. To check the consistency, 14 samples were annealed and oil quenched within $\pm 12^\circ\text{C}$ of these temperatures at 4°C increments. 4°C increments were decided to be suitable as experimental system has a tolerance of $\pm 2^\circ\text{C}$. After a detailed metallographic inspection on these samples, A_1 as 720°C and A_3 as 896°C were approved.

In order to show the feasibility of MBN measurements for industrial dual phase steels having lower (20-25 %) MVF [11], the experimental annealing was conducted with intercritical annealing temperatures (ICAT) close to A_1 . On the other hand, the chemical composition of the material used in these experiments did not allow producing a MVF much lower than 25% because of the unwanted carbide formation due to carbon content.

Sample production was conducted in order to have a descriptive plot of ICAT versus MVF using different annealing temperatures. MVF values were obtained from arithmetical means of values derived from the 5 images of 500x magnification taken from different points on the samples. The martensite volume fraction was determined Leica QM550MW Imaging System on metallographic sections etched in nital. The resulting plot is given in Figure 3.5.



a) AISI 8620 Ferrite+Pearlite



b) AISI 8620 ~100% Martensite

Figure 3.3 Initial microstructures prior to intercritical annealing

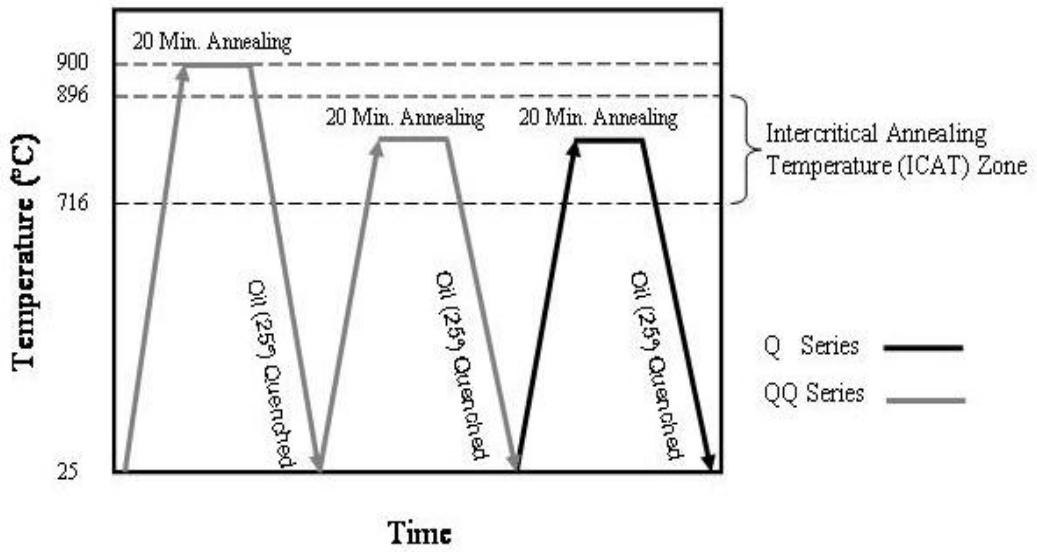


Figure 3.4 Summary of heat treatments

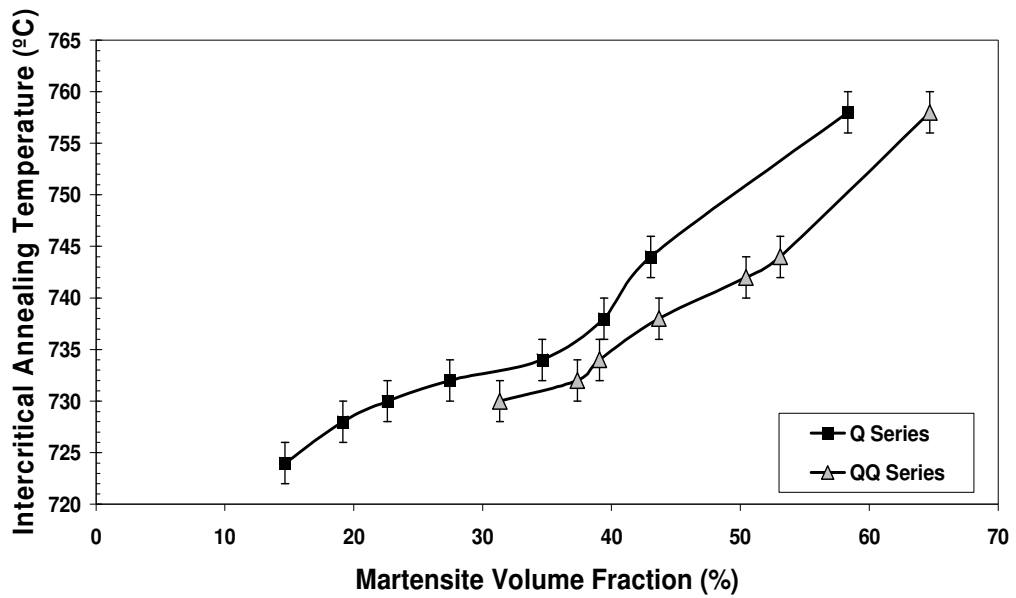


Figure 3.5 Variation of the martensite volume fraction depending on the initial microstructure (Q, QQ), and intercritical annealing temperature (ICAT).

3.5 Metallographic Inspections

Heat treated samples of 13.2 mm in diameter and 5 mm in thickness were prepared for metallographic inspection with standard grinding and polishing techniques. To eliminate effect of the decarburized layer formed during heat treatment, at least 0.5 mm of material was removed from the surface of the sample by grinding.

All samples are etched using 2% Nital (%2 HNO₃ + %98 C₂H₅OH). After etching, martensite was observed as light brown and ferrite as white in color during microscopic inspection. In order to see ferrite-martensite interface more clear a further etching with sodium meta bi-sulphite (%3 Na₂S₂O₅ + %97 H₂O) was applied. At the final stage martensite was observed as dark brown.

Leica QM550MW Imaging System was used for the optical metallographic investigations whereas Jeol JSM 6400 was used for the scanning electron microscopy.

3.6 Mechanical Tests

For tension testing ASTM E8M Standard specifications govern the parameters. Five tension test samples of each group were prepared by a CNC machine. Figure 3.6 shows the dimensions of the tension test specimens.

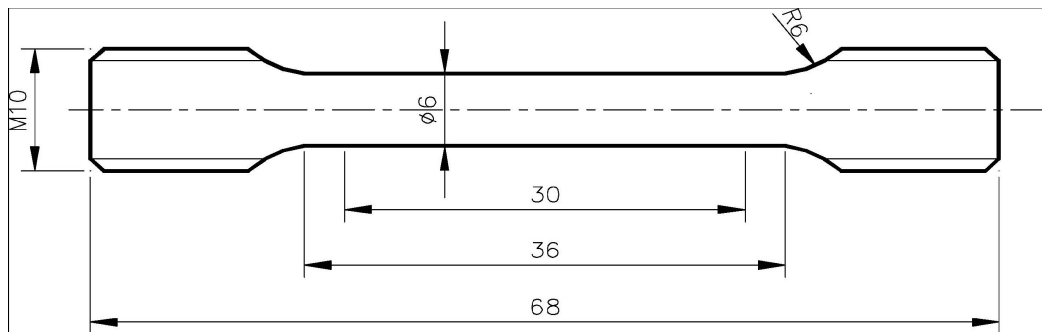


Figure 3.6 Dimensions of the tension test specimen

Hardness of the specimens (HRC) was measured by Instron Wolpert hardness tester using a 150 kg load. The hardness values given are the average of at least five measurements on each sample, with the total scatter being no more than ± 2 HRC.

3.7 Magnetic Barkhausen Noise Measurement

Any residual magnetism in the specimens was absent since all were heated at temperatures which are above the Curie temperature. Barkhausen noise signal was measured with μ SCAN 500-2 equipment (Figure 3.7 and 3.8). Measurements were carried out by using the sensor, S1-138-13-01. The central unit has two sensor connectors: Rollscan and μ SCAN. In this study, measurements were carried out using both sensor connectors.

In Rollscan measurements, the magnetizing frequency was 125 Hz and the filter passed frequencies from 70 to 200 kHz. In μ SCAN measurements, an excitation magnetic field with a frequency of 125 Hz was obtained. Magnetizing voltage, which adjusts the magnitude of magnetizing field applied to the specimen, was set to 10 V. Sampling frequency, the parameter determining how many samples per second are stored for signal analysis was set as 2 MHz. Number of bursts, the parameter determining how many magnetizing half cycles will be stored for signal analysis, was set as 186, the highest possible number of half cycles when the magnetizing frequency is 125 Hz and the sampling frequency is 2 MHz. The measured Barkhausen emission signals were filtered (pass-band: 0.1-1000 kHz) and amplified (voltage gain of 20 dB), and are plotted as a function of the magnetizing field over a hysteresis cycle in order to produce a MBN profile.

In order to be able to see the effect of frequency on Barkhausen noise measurements, Barkhausen noise response of a group of specimens were measured by setting the magnetizing frequency first to 125 Hz, then to 50 Hz and finally to 5 Hz. Number of bursts was set as 186 when the magnetizing frequency was 125 Hz, as 74 when the magnetizing frequency was 50 Hz and as 6 when the magnetizing frequency was 5 Hz. The other parameters remained the same.

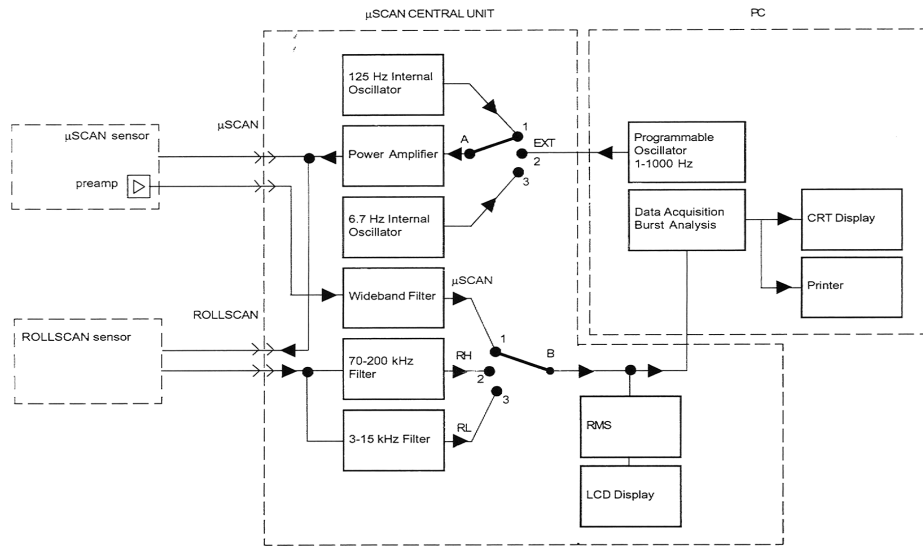


Figure 3.8. Block diagram of μSCAN 500 system.

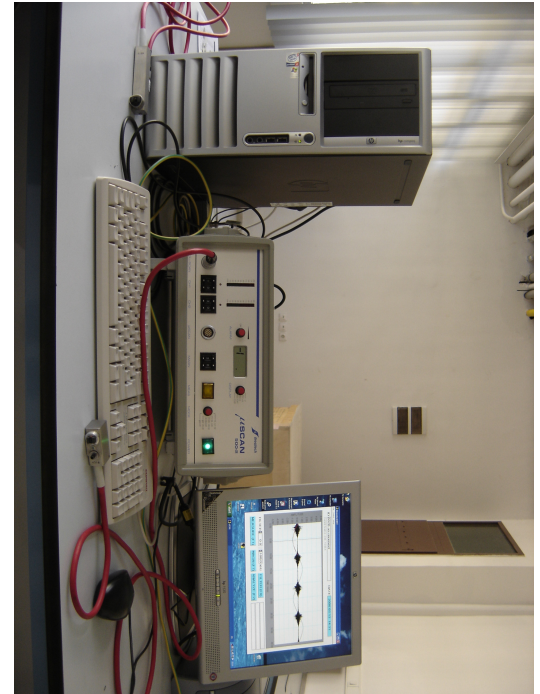


Figure 3.7 μSCAN equipment.

CHAPTER 4

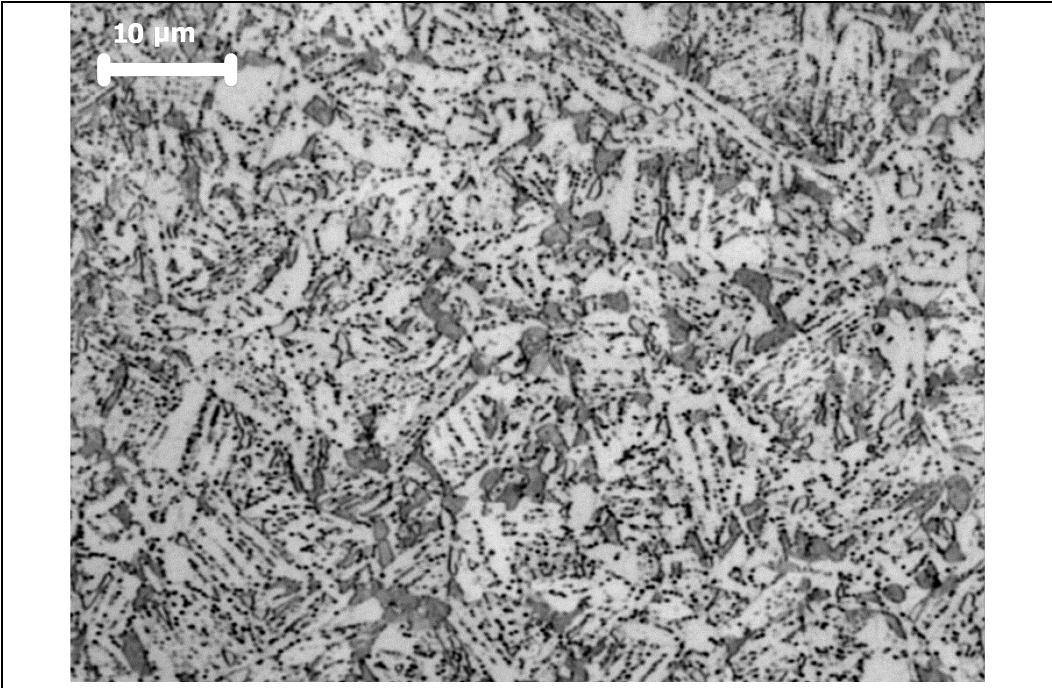
RESULTS AND DISCUSSION

4.1 General

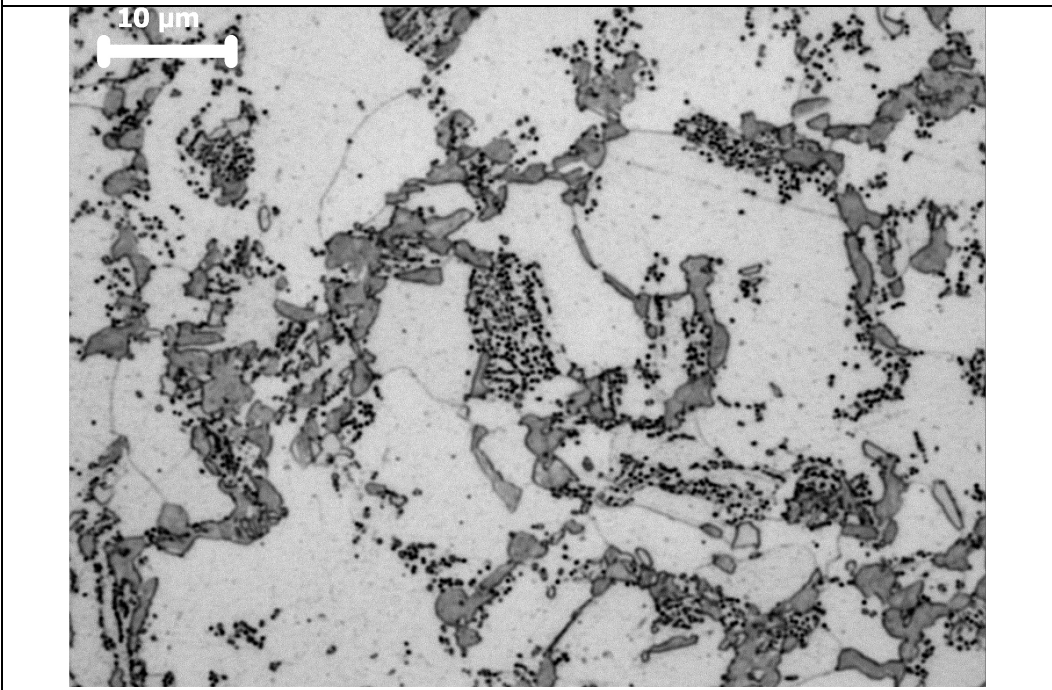
Samples having similar microstructural properties to those of industrial dual phase steels were produced from AISI 8620 steel. Equivalent results were achieved to those studies analyzing the applicability of MBN to dual phase steels and decisive correlation was established as well. In order to attain a high certainty in the MBN measurements, steel samples with low carbon content and having as homogenous microstructure as possible were chosen to avoid unexpected carbide formation during heat treatment. All samples have certainly same chemical composition being cut from a single piece of rod having a length of 6 meters.

At prior studies the results obtained on ferrite–martensite steels have to be extended to Dual-Phase steels with a lower martensite volume fraction, in order to show the feasibility of using such techniques for a non destructive characterization of industrial DPS [12].

Martensite volume fraction was achieved to be ~20% similar to those of industrial dual phase steels. However, some carbide formation was also observed which may adversely affect the mechanical properties of the sample and hence MP and RMS values. Optical micrographs with 1000X and SEM micrographs with 2500X and 5000X magnification in Figure 4.1 and Figure 4.2 show Carbide in between and in the vicinity of martensite islands.



a) QQ724 AISI 8620



b) Q724 AISI 8620

Figure 4.1 Micrographs showing low MVF and carbide formation

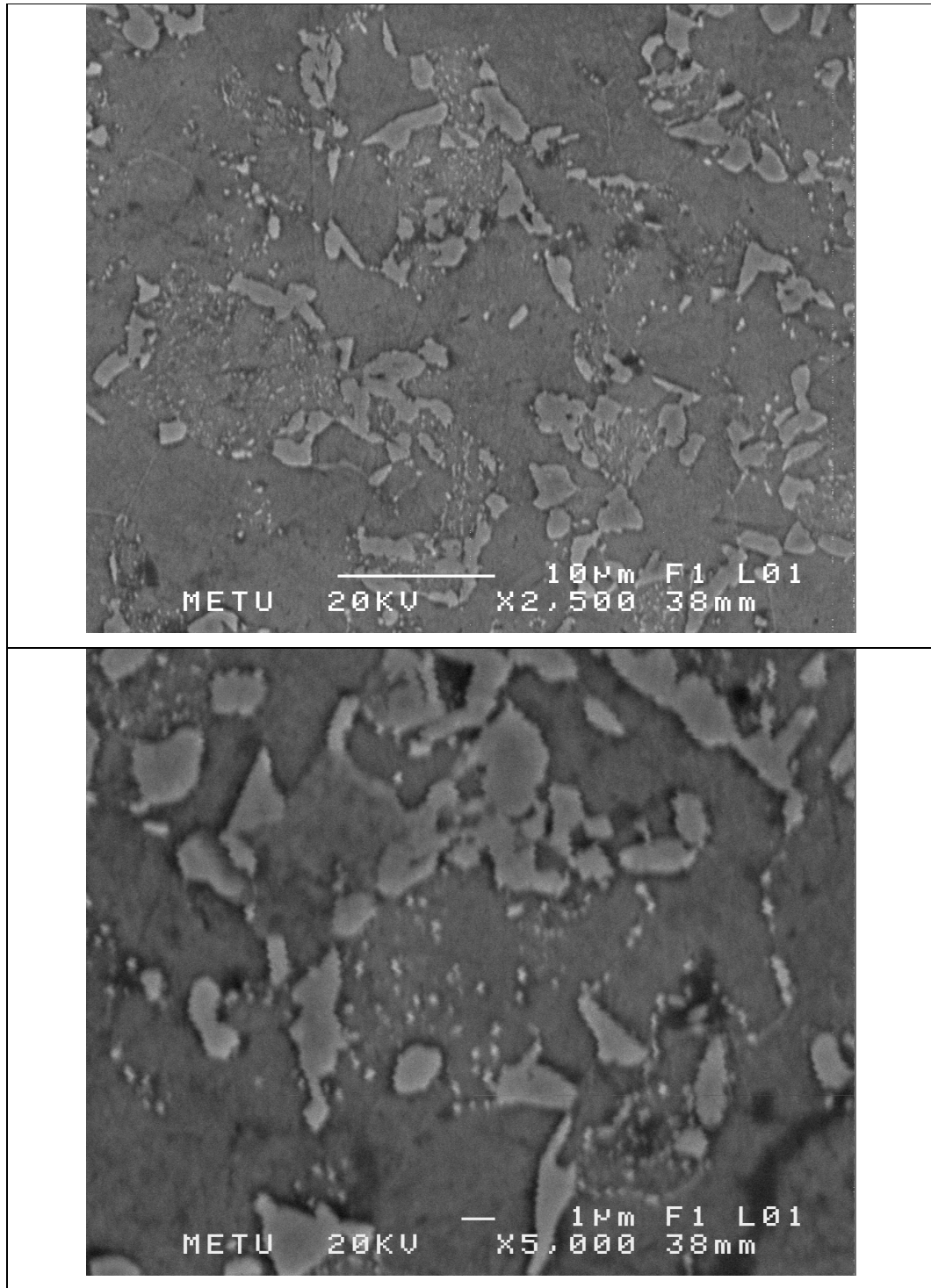


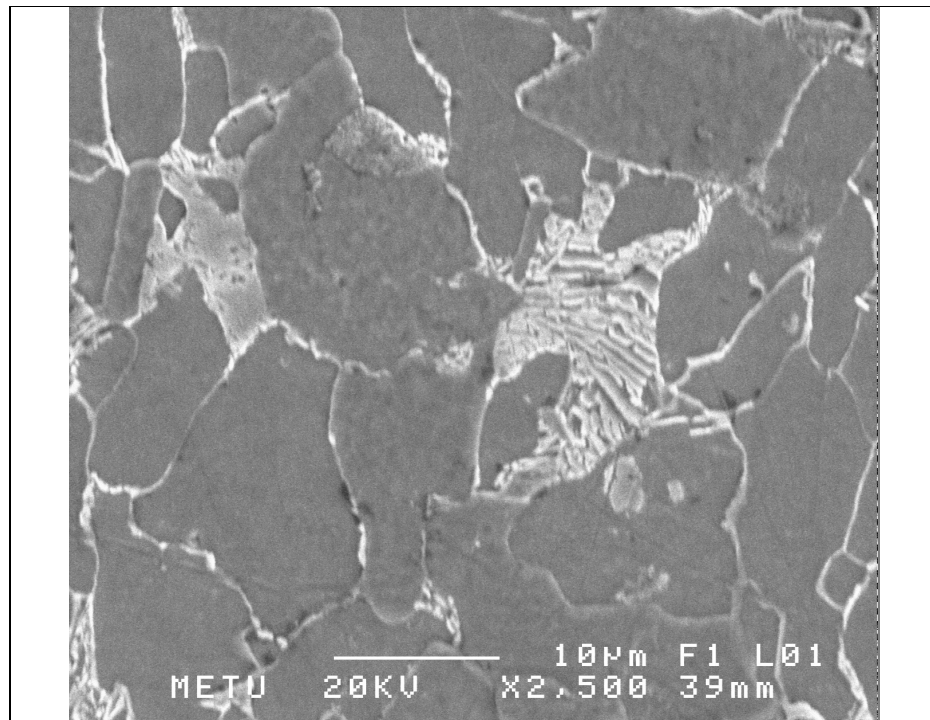
Figure 4.2 SEM micrographs of Q724 specimen showing carbide formation in AISI 8620 specimen

4.2 Results of Microstructural Investigation and Hardness Measurements

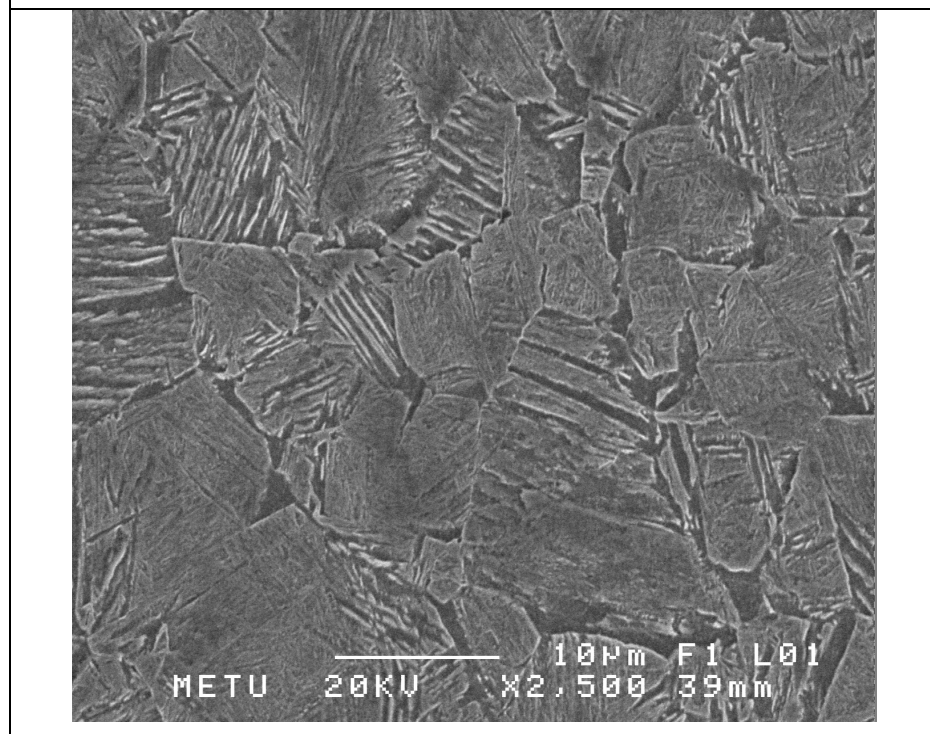
The austenite transformation following intercritical annealing is different from that after normal austenitisation in two respects. Firstly in dual phase heat treatment austenite volume fraction and its carbon content are determined by the ICAT. Under paraequilibrium condition (short intercritical annealing time) carbon, but not substitutional alloying elements segregates and determines phase proportions and compositions. Secondly a nucleation step is not required for new ferrite to form during cooling, because the old ferrite present during annealing can grow epitaxially into the austenite [18].

The SEM micrographs of the as-received and quenched-tempered samples are given in Figure 4.3. It is clearly seen that the as-received sample consists of ferrite and pearlite whereas quenched and 230°C-tempered sample has fully martensitic structure.

Figure 4.4 and Figure 4.5 show the micrographs of the AISI 8620 samples showing the variation in the martensite volume fraction depending on the starting microstructure (Q, QQ) and ICAT.



a) As-Received (AR) 8620



b) Quenched +Tempered (QT)

Figure 4.3 SEM micrographs of the as-received (AR) 8620 and quenched + tempered (QT) samples of AISI 8620

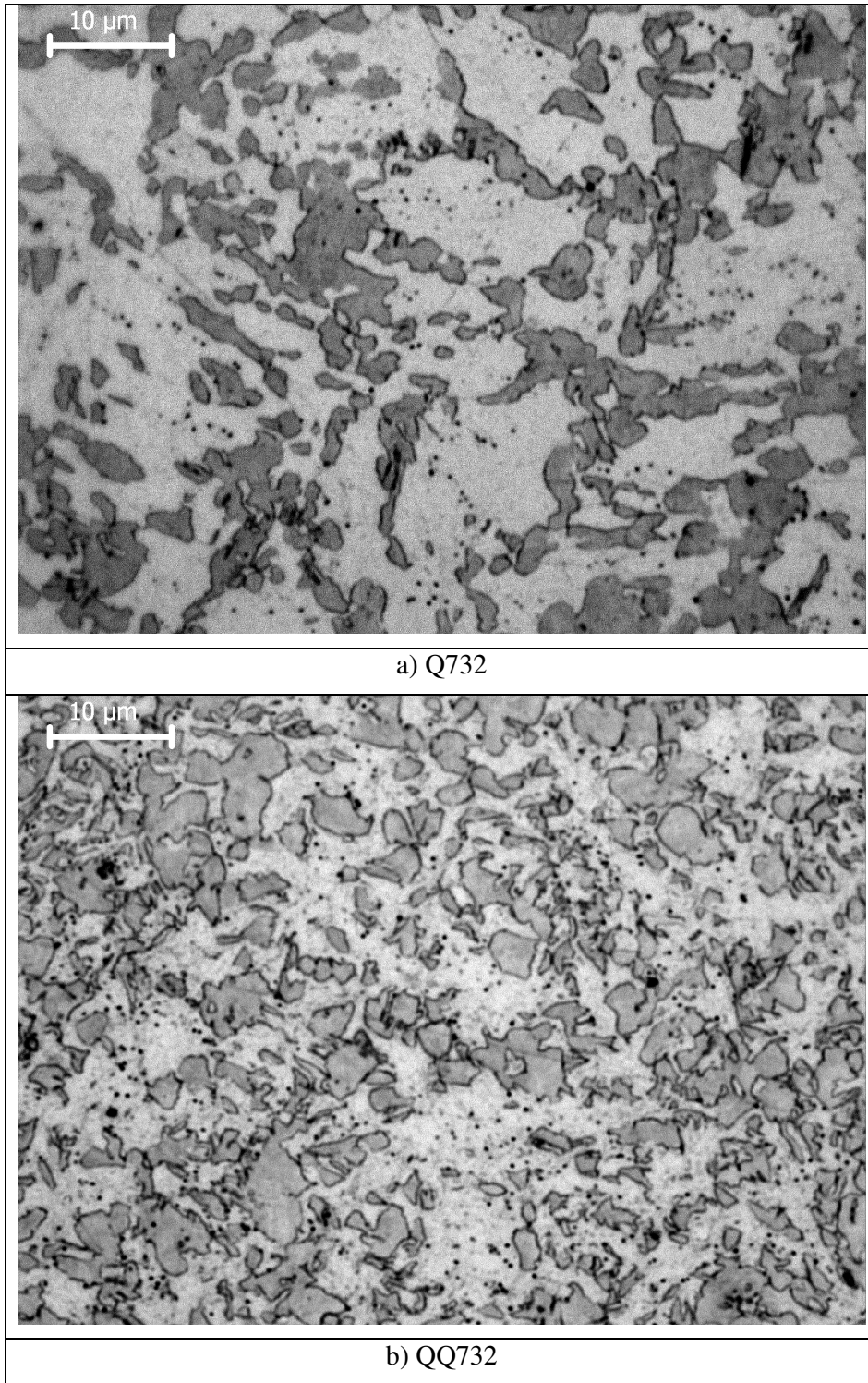
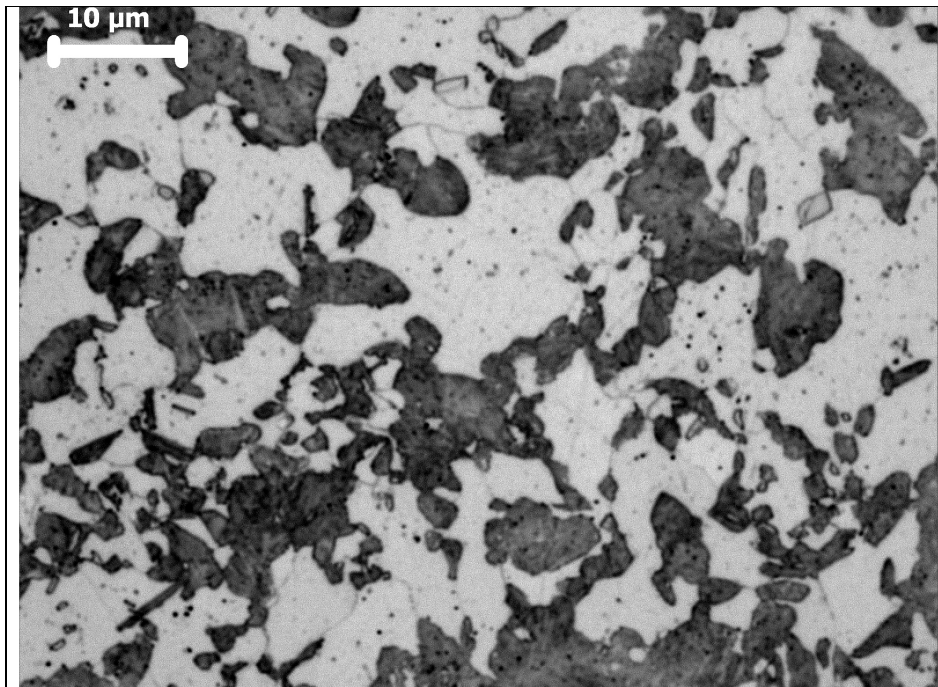
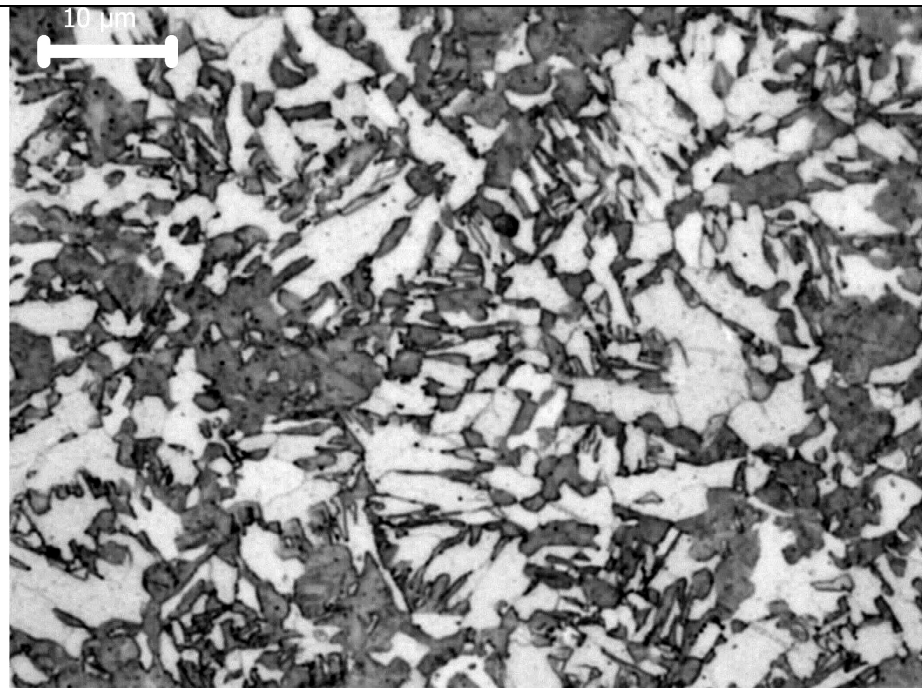


Figure 4.4 Optical micrographs of the AISI 8620 samples showing the variation in the martensite volume fraction depending on the starting microstructure (Q, QQ) and intercritical annealing temperature (ICAT).

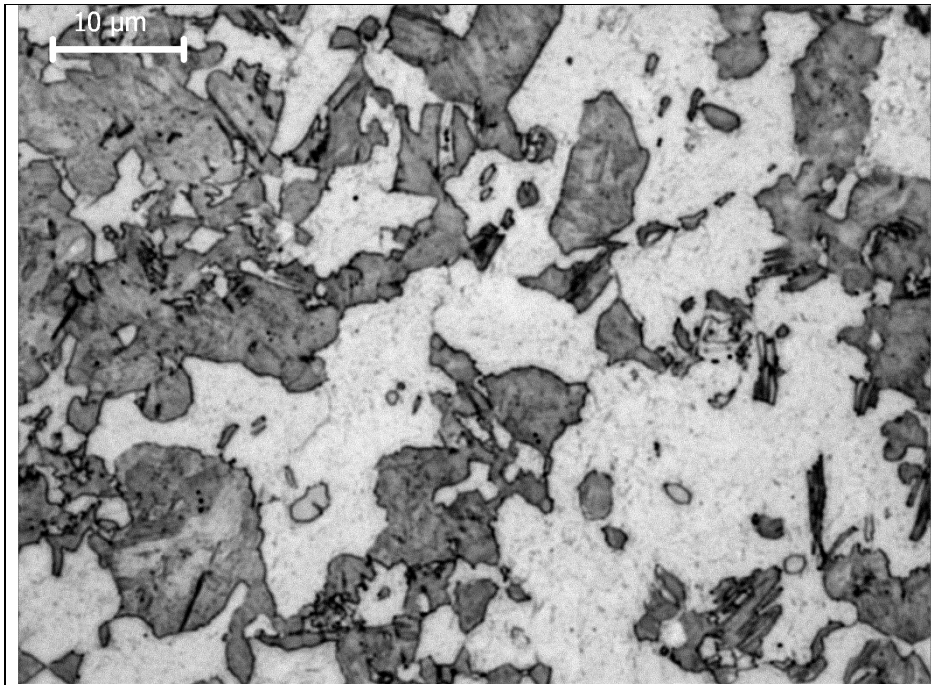


c) Q 738

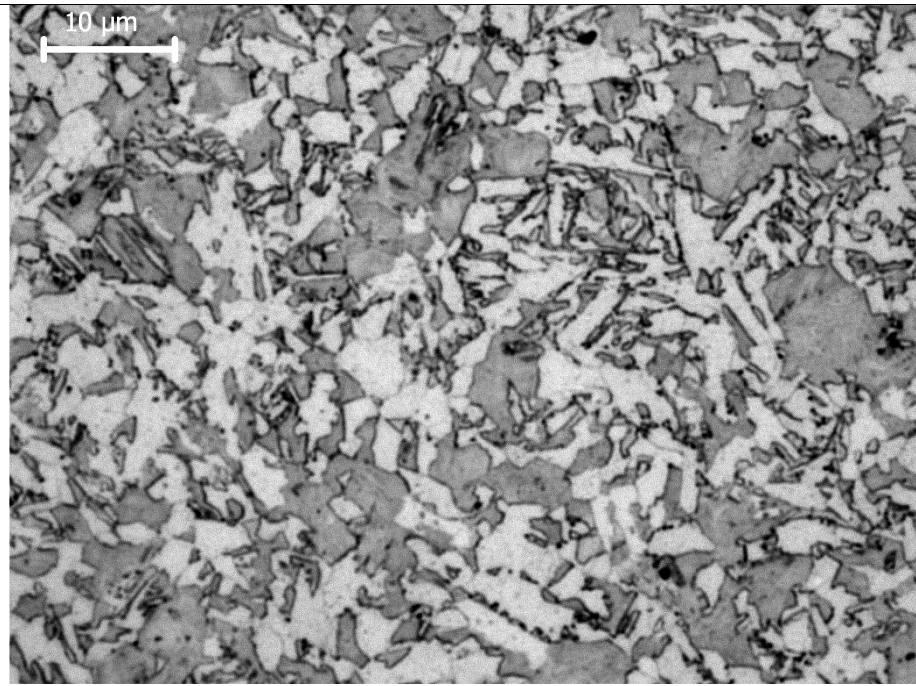


d) QQ 738

Figure 4.4 (Continued) Optical micrographs of the AISI 8620 samples showing the variation in the martensite volume fraction depending on the starting microstructure (Q, QQ) and intercritical annealing temperature (ICAT).



e) Q758



f) QQ758

Figure 4.4 (Continued) Optical micrographs of the AISI 8620 samples showing the variation in the martensite volume fraction depending on the starting microstructure (Q, QQ) and intercritical annealing temperature (ICAT).

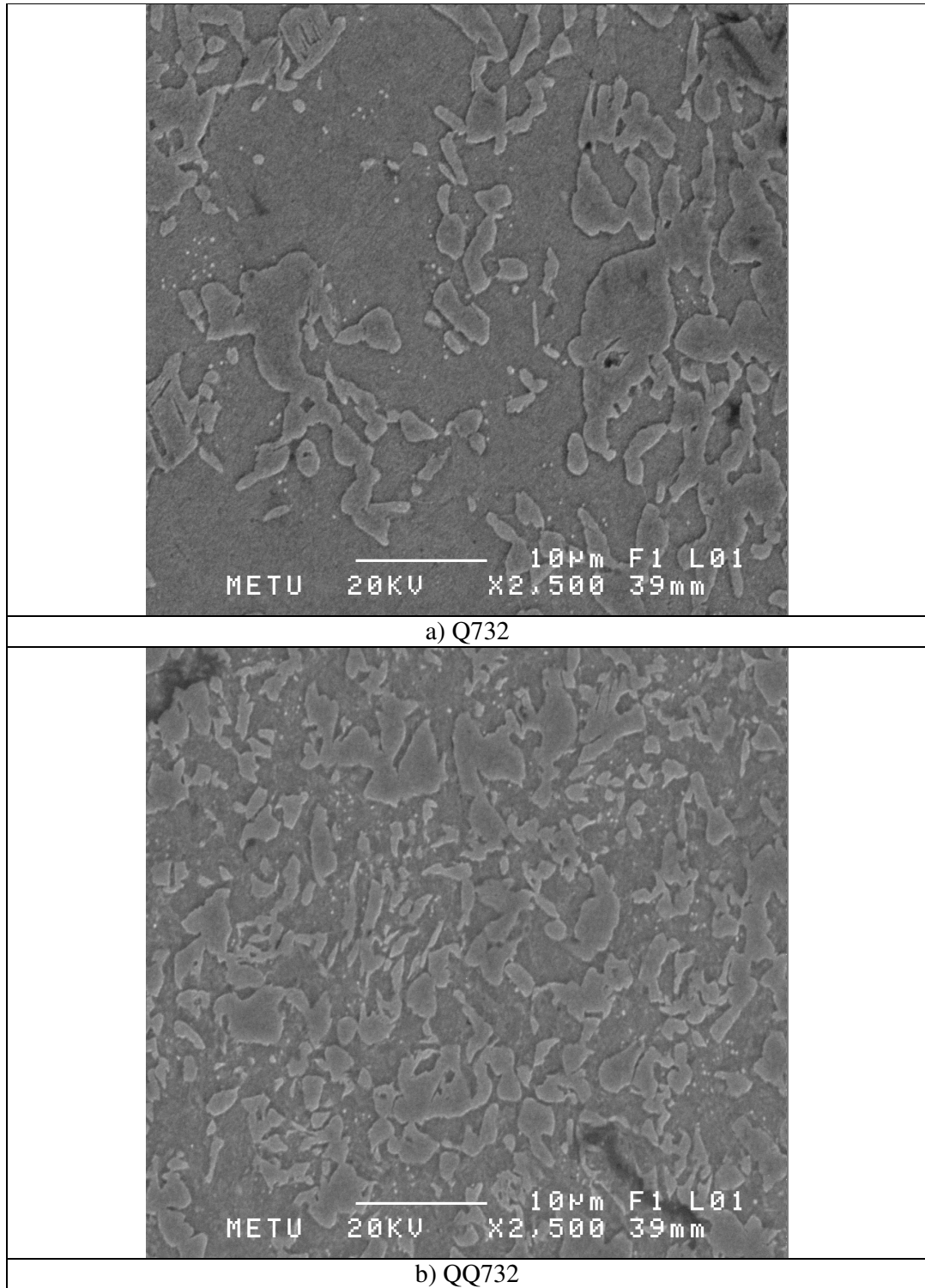


Figure 4.5 SEM micrographs of the AISI 8620 samples showing the variation in the martensite volume fraction depending on the starting microstructure (Q, QQ) and intercritical annealing temperature (ICAT).

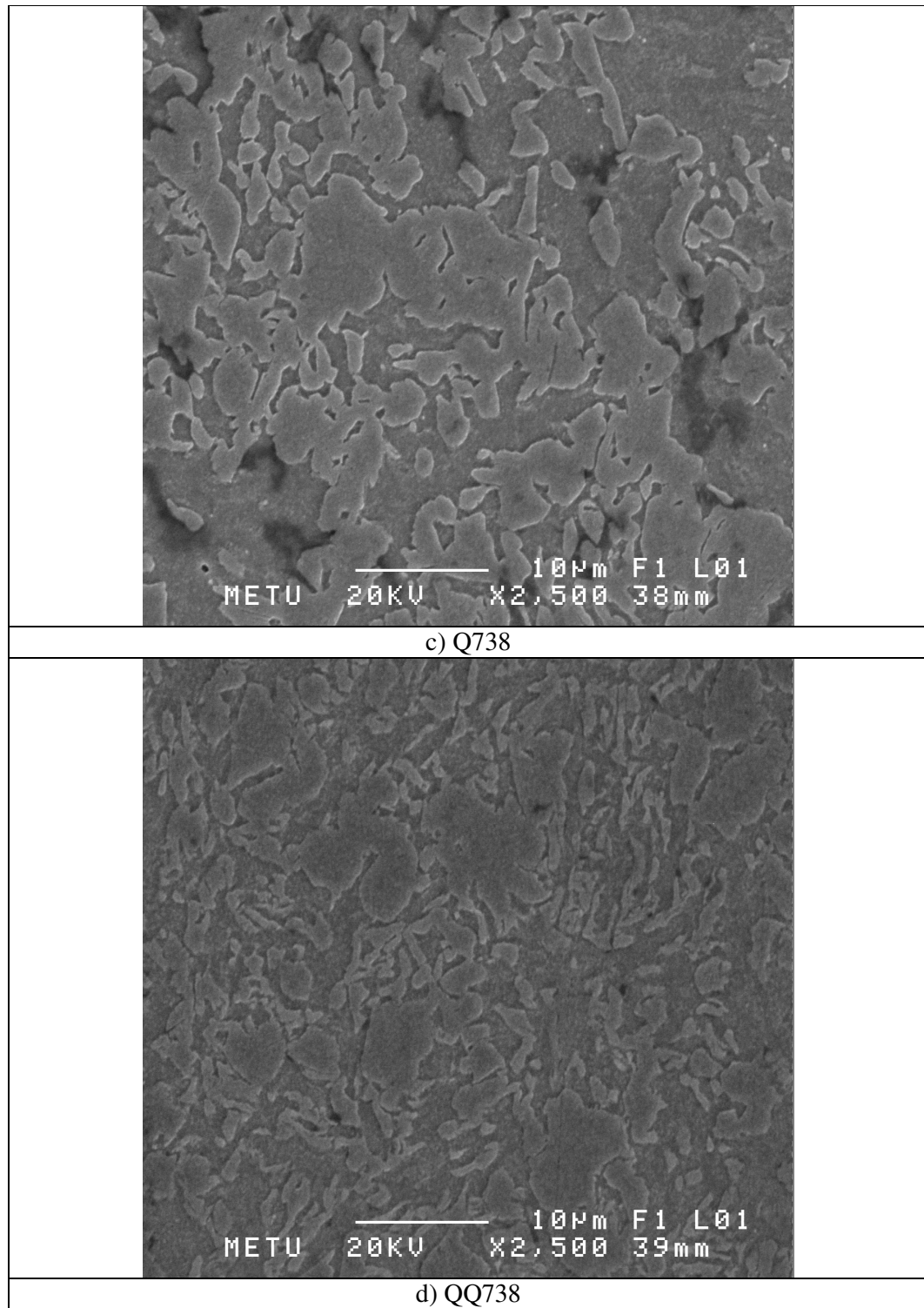
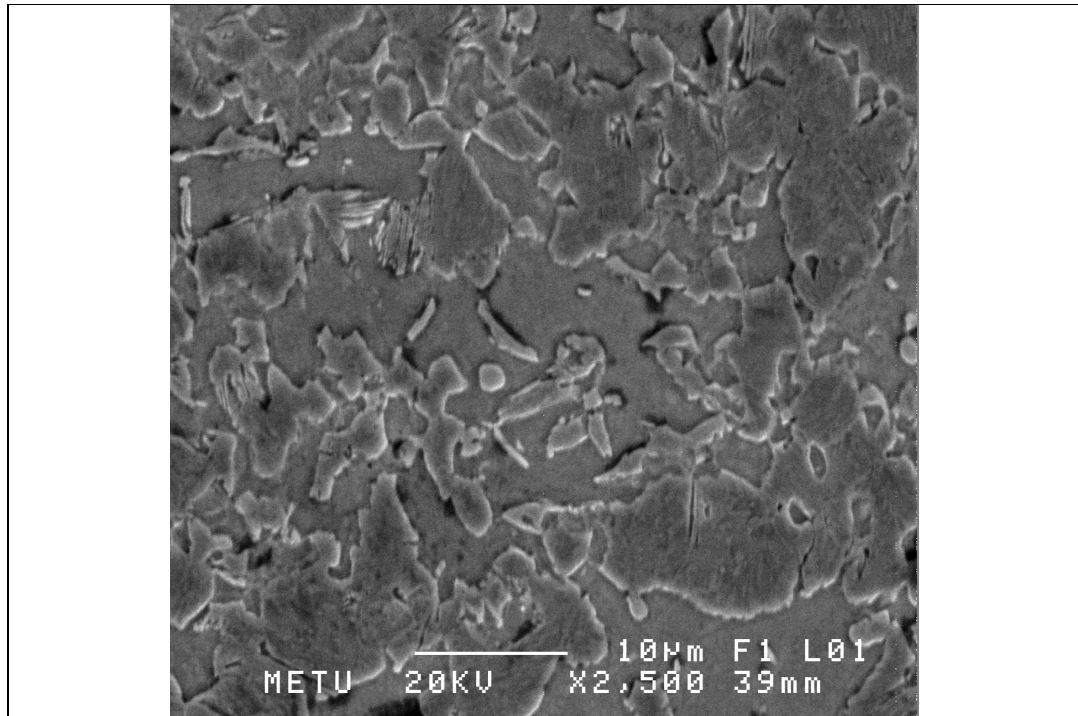
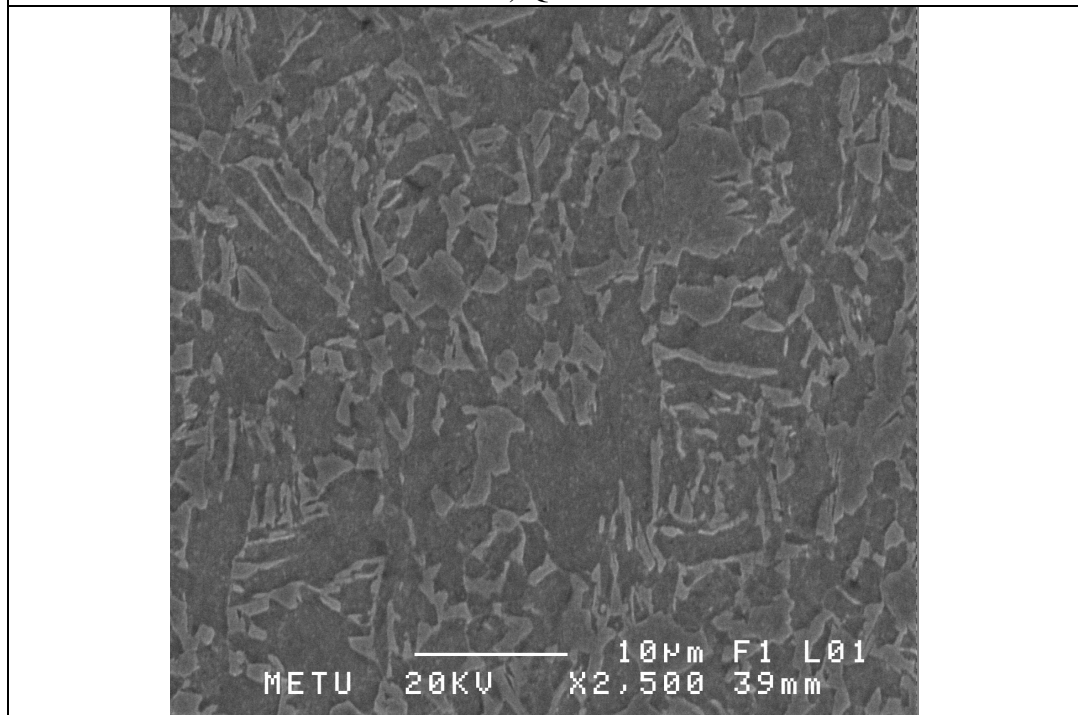


Figure 4.5 (Continued) SEM micrographs of the AISI 8620 samples showing the variation in the martensite volume fraction depending on the starting microstructure (Q, QQ) and intercritical annealing temperature (ICAT).



e) Q758



f) QQ758

Figure 4.5 (Continued) SEM micrographs of the AISI 8620 samples showing the variation in the martensite volume fraction depending on the starting microstructure (Q, QQ) and intercritical annealing temperature (ICAT).

The amount of austenite increases with increasing ICAT. As a result, the hardness of steel increased with increase in martensite content. Table 4.1 shows the hardness values of samples due to applied annealing temperature and as the martensite volume fraction resulted after annealing. MVFs targeted as 25%, 40% and 60% was achieved efficiently.

Table 4.1 ICAT, MVF and hardness values of samples.

Sample Code	ICAT (°C)	Aimed MVF (%)	Measured MVF (%)	Hardness (HRc)
AR	-	-	-	20.8
Q732	732	25	27.46±2.6	21.3
QQ732	732		37.34±1.5	24
Q738	738	40	39.42±2.3	23.5
QQ738	738		43.68±2.6	26.8
Q758	758	60	58.34±3.7	26.3
QQ758	758		64.69±1.9	31.1
QT	900	100	~100	35.9

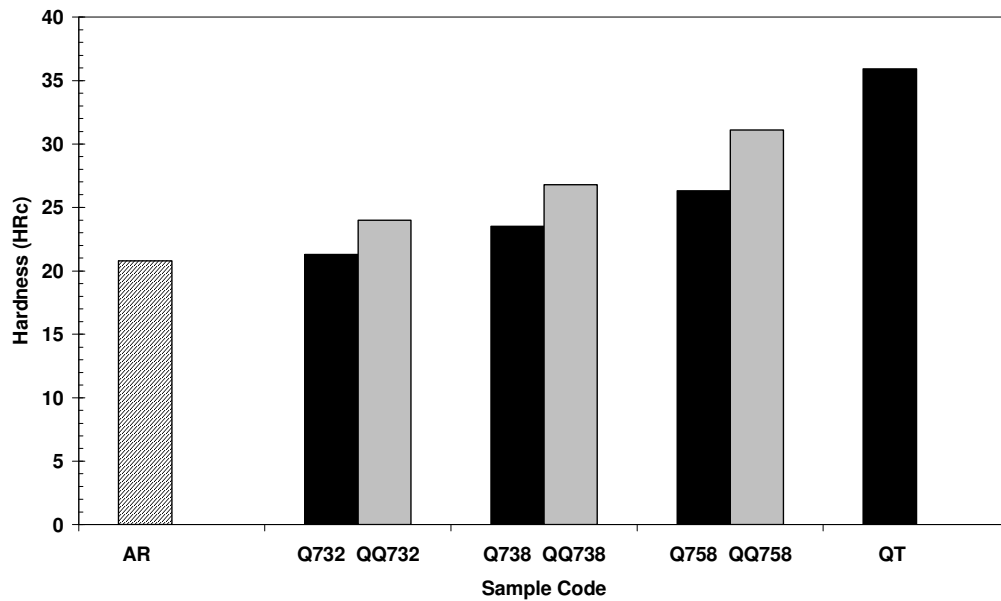


Figure 4.6 Variation of hardness values of the AISI 8620 samples depending on the starting microstructure (Q, QQ) and intercritical annealing temperature (ICAT).

The amount of austenite which transforms to martensite during quenching increases with increasing ICAT. As a result the hardness and strength of steel increased with increase in martensite content.

QQ series samples constitute higher hardness values as compared to those of Q series heat treated at the same ICAT. This can be explained by higher MVF and finer martensite morphology which is dependent upon the starting microstructures. It has been reported that fine initial structure produced more martensite than the coarse microstructure after annealing at low temperature and particular at the slower cooling rates. The reason for this was considered to result from higher carbon enrichment effect in the fine structure than the coarse ones during cooling. [16]. Therefore higher hardness values are observed for samples having finer microstructures than coarser microstructures (Figure 4.6).

4.3 Results of Tension Tests

The results of the tension test are given in figures 4.7 to 4.9. The samples of QQ series showed lower yield strength and UTS values than those of Q series. In contrary, Q series showed lower % elongation values for lower MVF, but at higher MVF Q series and QQ series have nearly the same elongations. As-received samples have the lowest values for yield and tensile strength and % elongation. QT samples have the maximum % elongation, but lower yield and tensile strengths than those of the DPS samples. Both Q and QQ series samples showed maximum yield strength values at about 40% MVF, and UTS of each series increase with increasing MVF. % elongation of QQ series decreased with increasing MVF whereas % elongation of Q series increased with increasing MVF.

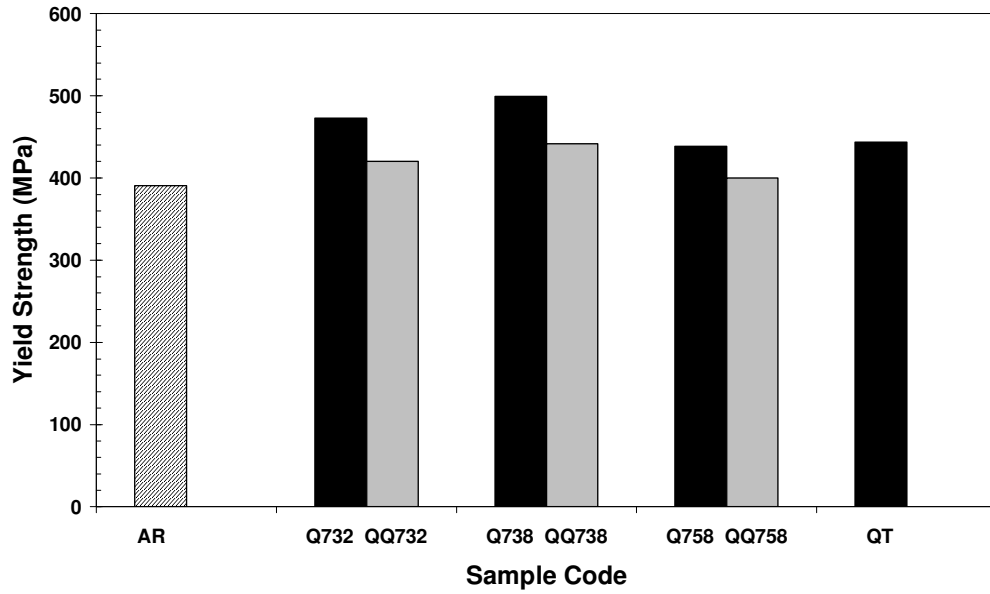


Figure 4.7 Variation of yield strength of the AISI 8620 samples depending on the starting microstructure (Q, QQ) and intercritical annealing temperature (ICAT)

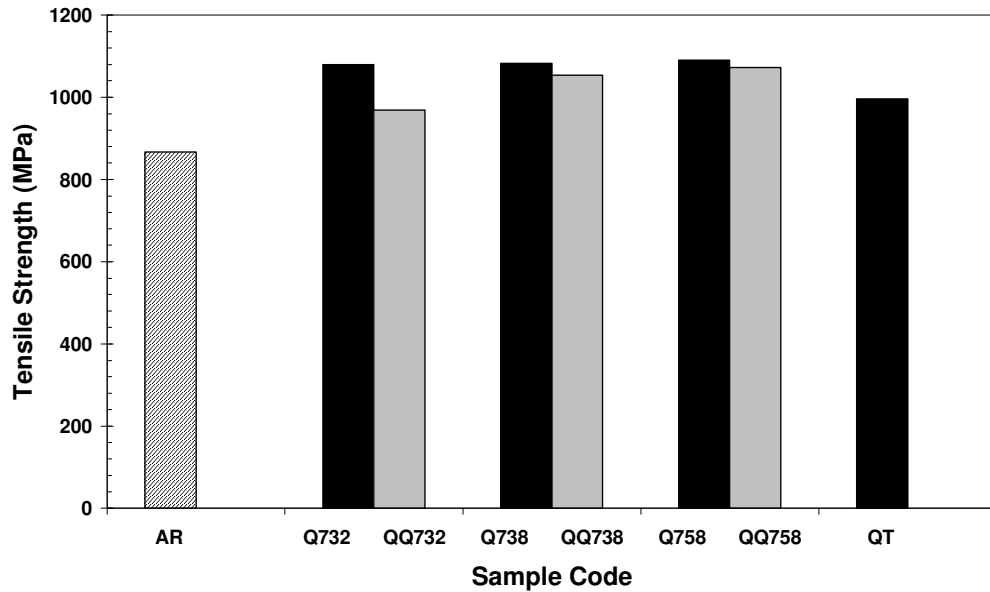


Figure 4.8 Variation of tensile strength of the AISI 8620 samples depending on the starting microstructure (Q, QQ) and intercritical annealing temperature (ICAT)

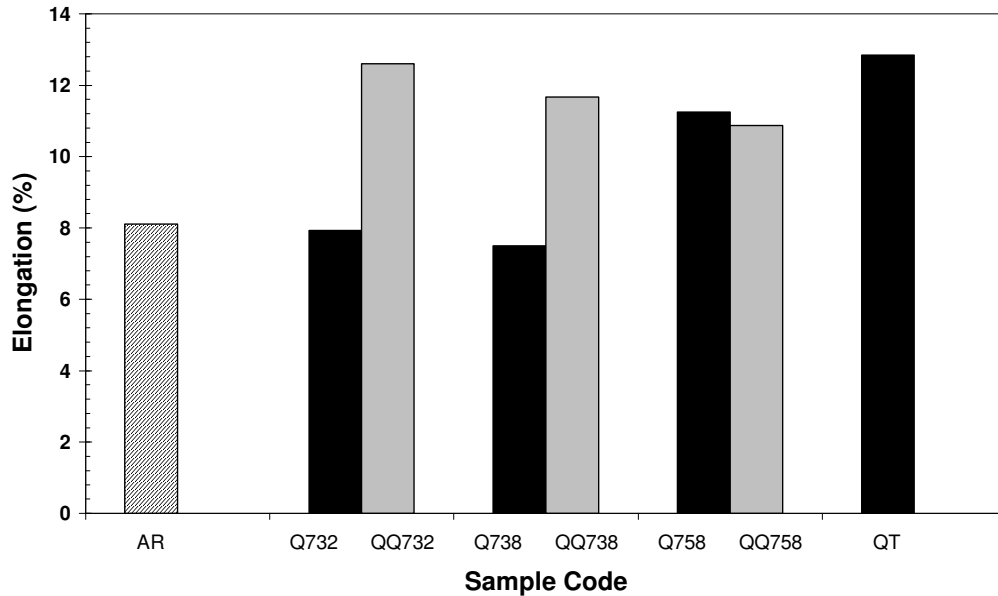


Figure 4.9 Variation of percent elongation of the AISI 8620 samples depending on the starting microstructure (Q, QQ) and intercritical annealing temperature (ICAT).

The mechanical properties of the two-phase alloys depend on a number of factors including phase chemistry and stability, volume fraction of the phases, strength ratio of the phases, and the morphology of the phases, including the grain size and orientation relationship. The yield strength depends on morphology of phases at a given volume fraction even though the chemistries of the phases remain constant. There are many factors that affect the plastic deformation behavior of a two-ductile phase alloy. Among the factors to be considered are the chemistries of the component phases, volume fraction and morphologies of phases, texture and crystallographic relationships between phases, inhomogeneous stress and strain distributions, and interaction stresses. Because of such complex factors, the “law of mixtures” rule to predict tensile properties of two-phase alloys can often not be applied. It is shown that the elastic interaction stresses and compatibility requirements between phases can result in a number of deformation mechanisms which are otherwise absent in the individual component phases. Similarly, in regard to the tensile ductility, the ductility of the two-phase material could be significantly lower than that predicted by the law of mixtures. There are a number of models

which make an attempt to understand such behavior, but it appears that more work is needed to understand both tensile and fracture behavior of two-phase alloys [38].

Sarwar and Priestner found that an increase in tensile strength could be obtained through an increase in martensite volume fraction as well as by an increase in the aspect ratio of martensite [15]. Tomita [16] and Bag et al. [17] have observed that equal amount of finely dispersed martensite phases exhibit the optimum combination of high strength and ductility; also the variation in tensile properties, such as the yield and tensile strength, and ductility with martensite content in the IQ (annealing/30 min at 920 °C and quenching (-7°C) + annealing/1h at intercritical annealing temperature and quenching) steels exhibit an unusual nature. The peak in tensile properties emerges due to finer microstructural constituents and due to the possible absence of average internal stress over the composite microstructure volume. For the effect of the starting microstructures, the results are also in agreement with those of Bayram A. et al, [39, 40] who have measured the mechanical properties of DPS after applying different heat treatments, MSA and MSB (Table 4.2). They concluded that with an initial martensite structure (MSB) optimum properties can be achieved.

Table 4.2 Mechanical properties of the samples

Heat Treatment	Yield Strength (MPa)	UTS (MPa)	Elongation %	Hardness
Q 732	473±50.6	1080±54.8	7.9±0.4	21.3±0.8 HRC
Q 738	499±28.7	1082±16.5	7.5±0.1	23.5±0.9 HRC
Q 758	439±21	1192±8	11.5±0.7	26.3±1.4 HRC
MSA [39, 40]	545±31.2	865±40.1	13.3	88 HRB
QQ 732	420±28.3	969±26.1	12.6±0.2	24±0.7 HRC
QQ 738	442±24.9	1053±4	11.7±0.2	26.8±1.6 HRC
QQ 758	400±24.6	1065±13	11	31.1±0.9 HRC
MSB [39, 40]	445±25.4	729±24.4	18	92 HRB

* At MSA (Intercritical Annealed Material): equiaxed martensite phase surround ferrite grains.

* At MSB (Step-Annealed Material): fine needle-like martensite phase distributed in the ferrite matrix.

The initial martensite structure, which is transformed to ferrite and austenite during the intercritical annealing stage, provides sufficient heterogeneous nucleation sites for austenite at prior austenite grain boundaries during this stage. The ferrite formation was presumably a process of recovery, recrystallization, and grain growth, which can lead to sub grain distribution in the ferrite. Parallel narrow laths within a prior austenite grain can bring about a fine dispersion of acicular martensite in a ferrite matrix upon quenching. Moreover, quenching from the two phase region gives rise to a high density of fresh dislocations in the ferrite grain due to the accommodation strain caused by the austenite-to-martensite transformations.

4.4. Results of Rollscan Measurements

Rollscan is a passive sensor which has a band pass filter with a range of 70-200 kHz. This filter range implies that the frequency components which are smaller than 70 kHz and those which are higher than 200 kHz are filtered off mathematically. Rollscan reads the magnetic parameter (MP) value of the specimens. Soft magnetic materials have a high magnetic response, whereas hard magnetic materials have a low magnetic response. Hence, a high MP value indicates that the specimen is a soft magnetic material, whereas a low MP value indicates that the specimen is a hard magnetic material.

Magnetic parameters derived from Barkhausen emission signals are strongly affected by the changes in the microstructure since the dimensions of the magnetic domains and the domain walls are comparable with the dimensions of such microstructural features as grain boundary, grains, precipitates, etc. Both, the domain wall movement and domain nucleation, are affected by the microstructural features.

Results of the Rollscan measurements are presented in graphical form in Figure 4.10. As-received sample (ferrite + pearlite) gave the highest value of MP. By the increase in MVF the MP values decreases proportionally. It can be easily seen from SEM pictures (Figure 4.5) that the volume fraction and morphology of martensite changes with changing initial microstructure and ICAT.

Due to the small size of martensite needles, the domain wall energy plays an important role, so the relative volume occupied by a wall is larger than in the other phases of steel (Figure 4.11). Domain walls are pinned due to high dislocation density; therefore the resistance to the growing domains is very high. Domain wall displacements are low and walls are difficult to create since the reversal of magnetization requires a strong field. Hence, the resulting MBN is very weak. Moreover, the second order internal stresses in the needles, which are inherent to the martensitic transformation, may also have an effect via the magneto-elastic coupling

The correlation between MP values and hardness is shown in Figure 4.12. There is a linear relationship, it is seen that the slopes of the curves are almost the same; however, the relative positions of the curves are different. It means that the effect of annealing temperature, which causes a change in the martensite content, is similar on both Q and QQ series samples. The increase in martensite content causes an increase in the hardness of the sample, while decreasing the MP value. Due to higher MVF at same annealing temperatures the QQ series have higher hardness values and lower MP values. A direct correlation between MP and MVF was established as shown in Figure 4.13. Points close to the center of samples of 13.2 mm in diameter and 5 mm in thickness was chosen for MVF measurements and MP measurements were made accordingly. Measurements taken at the points which are very close to each other will allow identify small volume fraction differences in industrial applications.

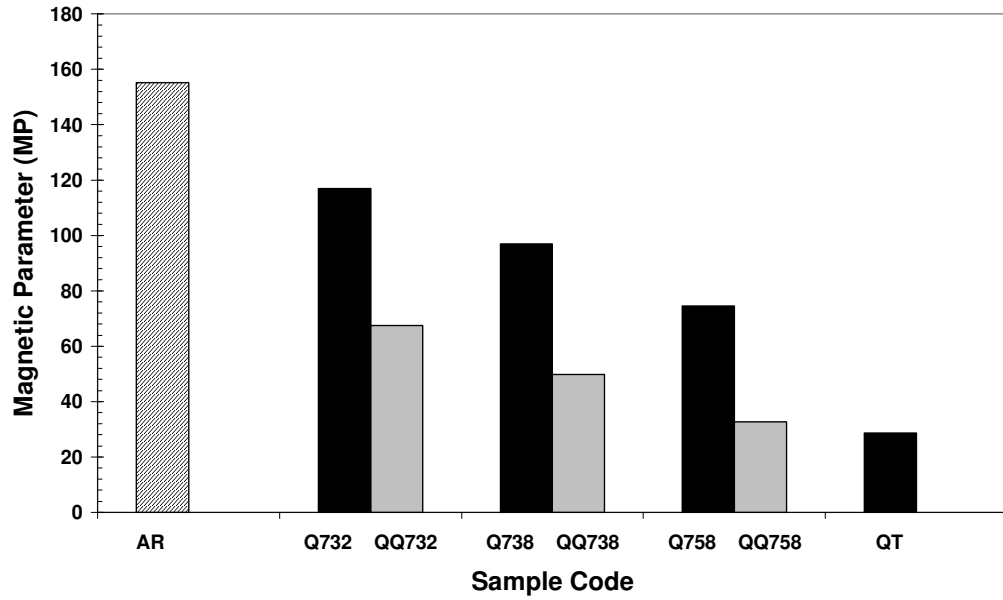


Figure 4.10 Variation of magnetic parameter of the AISI 8620 samples depending on the starting microstructure (Q, QQ) and intercritical annealing temperature (ICAT).

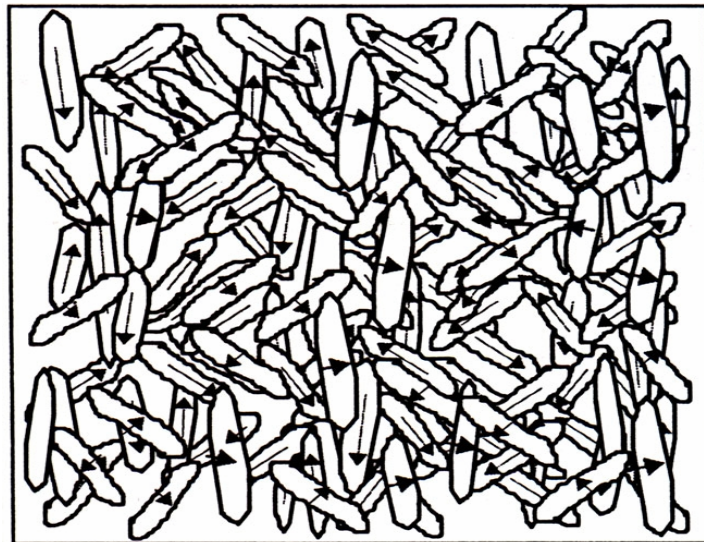


Figure 4.11 A sketch of magnetic domains in a martensitic microstructure.

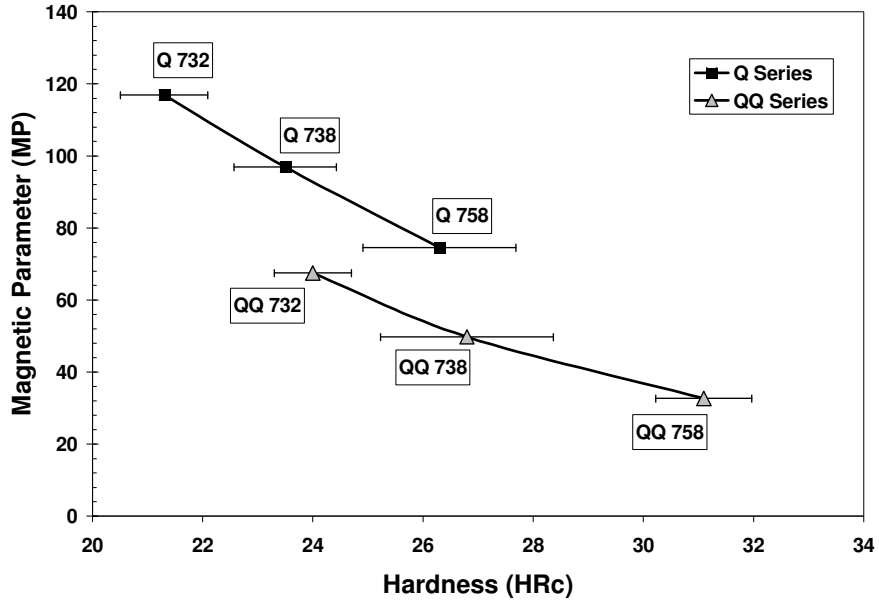


Figure 4.12 Correlation between magnetic parameter (MP) and hardness of the AISI 8620 samples

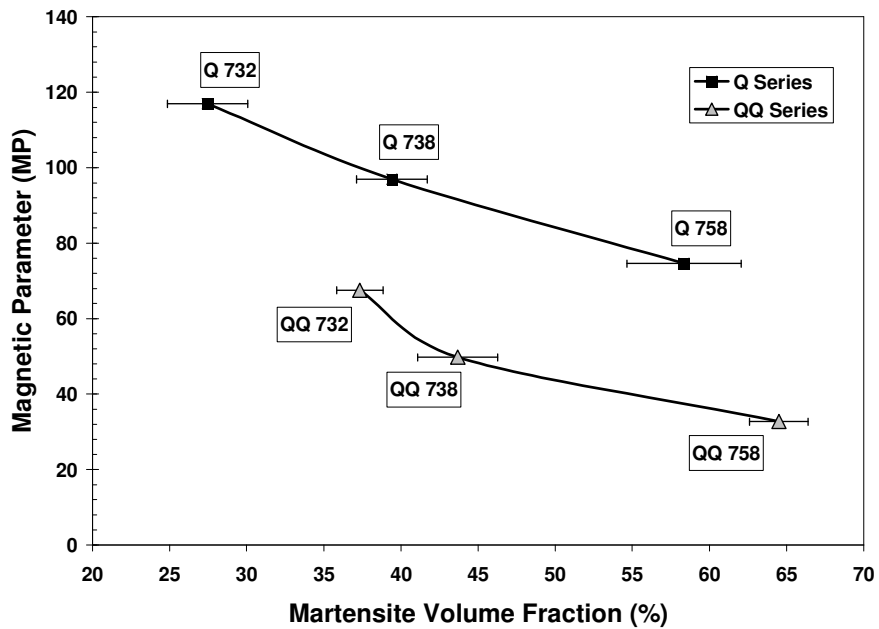


Figure 4.13 Correlation between magnetic parameter (MP) and martensite volume fraction (MVF) of the AISI 8620 samples

4.5. Results of μ SCAN Measurements

Under the effect of an alternating magnetic field, a magnetic hysteresis loop is induced in the volume measured due to the energy loss associated with the irreversible process of magnetisation. This irreversible process is strongly related to the dynamic behaviour of domains, i.e., nucleation, annihilation and growth of domains. This behaviour is affected by grain or lath boundaries, dislocations and precipitates. Consequently, the number of domain walls moving at a given instant and the mean free path of the domain wall displacement decide the MBN peak height.

When a ferromagnetic material is excited by an external magnetic field, the magnetization state of the sample exhibits a sequence of Barkhausen jumps. Magnetic Barkhausen emissions are detected in the form of voltage pulses induced in a sense pick-up coil positioned close to the surface of the material. The amplitude distribution of such pulses depends on the microstructure and residual stress. An analysis of the Barkhausen signal permits evaluation of changes in subsurface material condition. The root mean square (RMS) value of the voltage signal detected from the specimens is given as an output in μ SCAN measurements. RMS voltage, which is obtained by averaging the BE signal over the time for magnetization reversal, gives the average of the Barkhausen activity.

Figure 4.14 gives the correlation between RMS and hardness whereas Figure 4.15 shows the correlation between RMS and MVF of the AISI 8620 samples. As the MVF of the specimen, and consequently hardness increases the MBN peak height decreases. Under the effect of an external magnetic field, the resistance to the growing domains in martensite phase is very high since domain walls are pinned due to high dislocation density. Domain wall displacements are limited, and formation of the new domain walls is rather difficult since the reversal of magnetization requires a stronger field. Hence, the resulting MBN is very weak. Micro-residual stresses in the martensite needles may also have an effect via the magneto-elastic coupling.

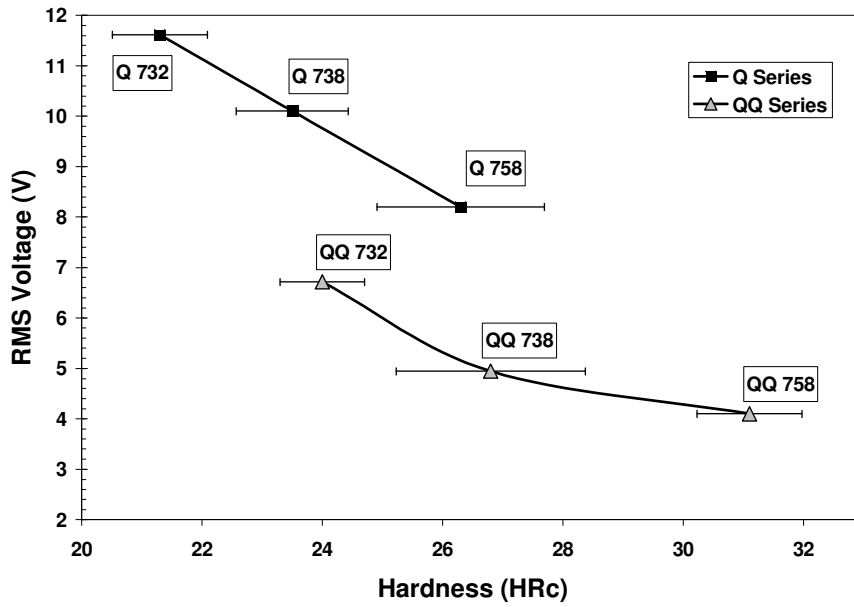


Figure 4.14 Correlation between RMS (V) and hardness (HRC) of the AISI 8620 samples

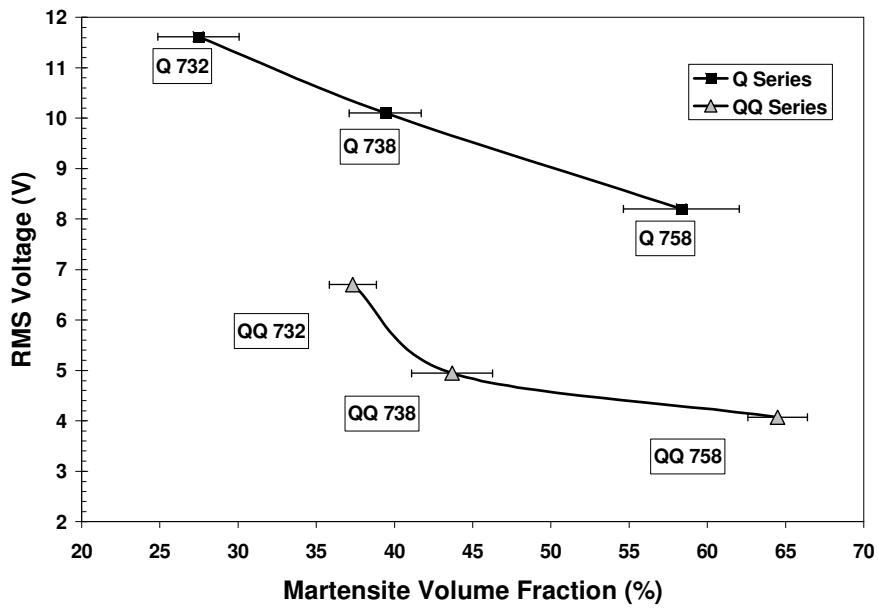


Figure 4.15 Correlation between RMS (V) and martensite volume fraction (MVF) of the AISI 8620 samples

The relative RMS voltage as a function of relative magnetic excitation is plotted on Figure.4.16 for all samples. The MBN for AR (ferrite + pearlite) steel shows the highest amplitude where QT samples have the lowest amplitude. However, by the increase at the MVF of samples the RMS values decrease for each series. The RMS voltage decreases prominently for QQ series compared with Q series intercritically annealed at the same temperature. Also, the position of the QQ series peaks move to a higher relative magnetic excitation as the result of finer microstructure.

The magnetic field at which the peak value of the MBN signal was located shifted to higher fields as the MVF of the specimen increased. The lower Barkhausen emission occurring at a higher magnetic field indicates an increase in the martensite content.

Soft magnetic materials reach their saturation magnetization with a relatively low applied field, i.e. they are easily magnetized and demagnetized. Whereas, hard magnetic materials have a high resistance to demagnetization and a large magnetic field must be applied in a direction opposite to that of the original field to reduce the magnetization of the specimen to zero after the specimen has reached its saturation magnetization. Thus, a signal peak that is close to zero relative magnetic excitation field in a MBN profile indicates that the specimen can be easily magnetized. On the other hand, the peak being far away from zero indicates that the specimen is hard to magnetize. Therefore, the increase in the relative magnetic excitation field can be considered as an evidence for the increase in martensite content.

It has been reported that tempering at about 200°C is mainly associated with the appearance of ϵ -carbides. The tetragonality of martensite starts to reduce. However, since the microstructure is still needle shaped, the morphology of the magnetic microstructure hardly changes. Therefore, the amplitude and peak position of the MBN signal is not deeply modified [31]. For this reason, the MBN profile of the quenched and 230°C tempered sample is very similar to the as-quenched samples, i.e., a signal peak with very low height and positioned at relatively high magnetic excitation fields.

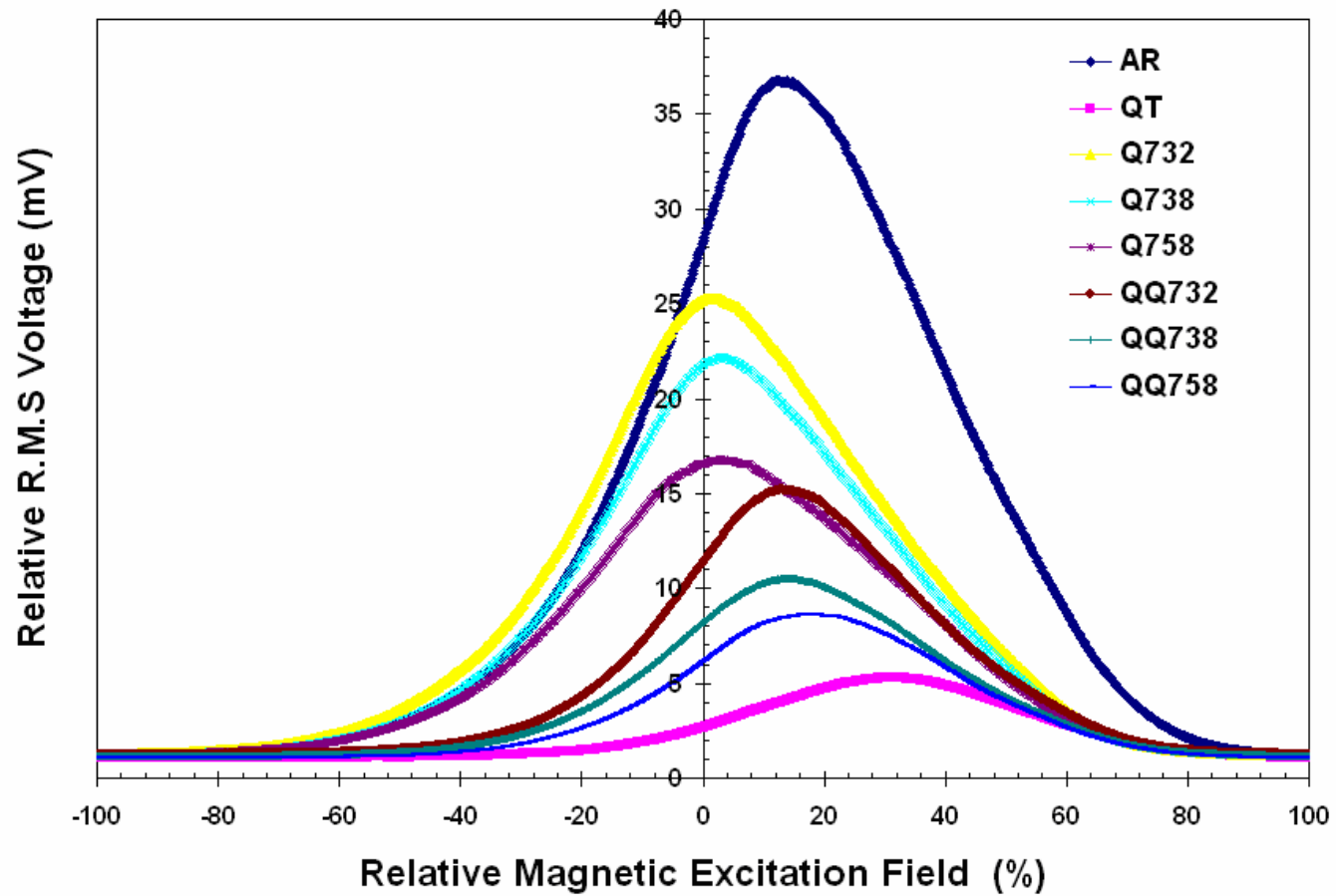


Figure 4.16 Relative RMS voltage as a function of relative magnetic excitation of the AISI 8620 samples

CHAPTER 5

CONCLUSIONS

By quenching of AISI 8620 specimens having two different starting microstructures (ferrite-pearlite and fully martensite), from various intercritical annealing temperatures (ICAT) namely 732°C, 738°C, and 758°C in the ferrite-austenite region, the microstructures consisting of different volume fractions of martensite and morphology have been obtained. The microstructures, strength properties and hardness values were determined by conventional metallographic and mechanical tests. The measurements of the Magnetic Barkhausen Noise (MBN) were performed by using both Rollscan and μ SCAN sensor connectors. After evaluating and comparing the results, the following conclusions can be drawn:

- The martensite content of the dual phase steels is dependent on the ICAT chosen.
- The initial microstructure affects the morphology and the amount of the martensite formed.
- The volume fraction and morphology of the martensite directly affect the hardness, mechanical strength and ductility of the dual phase steel.
- MBN method can be used for nondestructive characterization of dual phase steels.
- A good correlation between the martensite volume fraction, hardness and MBN emission has been obtained. MBN emission can be represented by the peak height and peak position of the MBN signal. MBN peak height decreases as the ICAT, therefore the volume fraction of martensite increases, also the position of the peak moves to higher relative magnetic excitation.

REFERENCES

1. U. S. Steel, www.ussautomotive.com/auto/tech/grades/dual_ten.htm, last visit Jan 2006.
2. R. D. Lawson, D. K. Matlock and G. Krauss: in “Fundamentals of dual-phase steels”; (ed. R. A. Kott and B.L. Bramfitt), 1981, AIME, New York, pp. 347-381.
3. Salzgitter Flachstahl, www.salzgitter-flachstahl.de/en/News/Archiv/2005/Dual_Phasen_in_feuerverzinkter_Ausfuehrung/, last visited on July 2006.
4. B. Engl, Forum Tech. Mitt. Krupp, July 2000, (1) 9-12.
5. D. Vanderschueren, In Proc. Conf. Thermomechanical Processing of Steels, London, 24-26 May, 2000.
6. T. Heller, In Proc. Conf. Thermomechanical Processing of Steels, London, 24-26 May, 2000.
7. G. E. Dieter, Mechanical Metallurgy (McGraw Hill, New York, 1961), p. 190
8. Plant Services Magazine, www.plantservices.com/articles/2006/075.html, last visited on July 2006.
9. Queen’s University, www.physics.queensu.ca/~lynann/mbnoise.html, last visited on December 2005.
10. D.R. Askeland, P.P. Phulé, The Science and Engineering of Materials, 4th ed.
11. Stresstech group, www.stresstech.fi., last visited on November 2005.
12. M. Blaow, J. T. Evans and B.A. Shaw, Acta Materialia 53 (2005) 279-287.
13. X. Kleber, A. Hug, J. Merlin and M. Soler, ISIJ International 44 (6) (2004) 1033-1039.
14. K. M. Ralls, T. H. Courtney and J. Wulff, Introduction to Materials Science and Engineering, 1976 John Wiley & Sons, New York.
15. M. Sarwar and R. Priestner, Journal of Materials Science 31 (1996) 2091-2095.
16. Y. Tomita, Journal of Materials Science 25 (1990) 5179-5184.
17. A. Bag, K. K. Ray and E. S. Dwarakadasa, Metallurgical Materials Transactions A 30 (1999) 1193-1202.

18. M. Erdogan, *Scripta Materialia* 48 (2003) 501-506.
19. A. P. Modi, *Tribology International* ARTICLE IN PRESS
20. V. Moorthy, S. Vaidyanathan, T. Jayakumar and B. Raj, *Journal of Magnetism and Magnetic Materials* 171 (1997) 179-189.
21. C. Gatelier-Rothea, J. Chicois, R. Fougères and P. Fleischmann, *Acta Mater.* 46 (1998) 4873-4882.
22. V. Moorthy, S. Vaidyanathan, T. Jayakumar and B. Raj, *Philosophical Magazine A* 77 (1998) 1499.
23. O. Saquet, J. Chicois and A. Vincent, *Materials Science and Engineering A* 269 (1999) 73-82.
24. J. Kameda and R. Ranjan, *Acta Metallurgica* 35 (1987) 1527-1531.
25. A.P. Parakka, D. C. Jiles, H. Gupta and M. Zang, *Journal of Applied Physics* 81 (1997) 5085-5086.
26. H. Gupta, M. Zhang and A. P. Parakka, *Acta Materialia* 45 (1997) 1917-1921.
27. J. Guathier, T. W. Krause and D. L. Atherton, *NTD & E International* 31 (1998) 23-31.
28. K. Mandal, Th. Cramer and D. L. Atherton, *Journal of Magnetism and Magnetic Materials* 212 (2000) 231-239.
29. B. Raj, V. Moorthy and S. Vaidyanathan, *Materials Evaluation* 55 (1997) 81.
30. J. Anglada-Rivera, L. R. Padovese and J. Capo-Sanchez, *Journal of Magnetism and Magnetic Materials* 231 (2001) 299-306.
31. C. H. Gür and İ. Çam, *International Journal of Microstructure and Material Properties* 1 (2006) 208-218.
32. C. H. Gür and İ. Çam, *Material Characterization* accepted for publication in 2006.
33. D-G. Park, C.G. Kim and J-H Hong, *Journal of Magnetism and Magnetic Materials* 215-216 (2000) 765-768.
34. J-H. Kim, D-G. Park, C-II Ok, E-Pak Yoon and Jun-Hwa Hong, *Journal of Magnetism and Magnetic Materials* 196-197 (1999) 351-353.
35. T. Okazaki, T. Ueno, Y. Furuya, M. Spearing and N. W. Hagood, *Acta Materialia* 52 (2004) 5169-5175.
36. M. Blaow, J. T. Evans and B. A. Shaw, *Journal of Magnetism and Magnetic Materials* 303 (2006) 153-159.

37. K.W. Andrews, *Journal of Iron & Steel Institute* 203 (1965) 721.
38. S. Ankem, H. Margolin, C. A. Greene, B.W.P. Neuberger and G. Oberson, *Progress in Materials Science* 51 (2006) 632–709
39. A. Bayram and A. Uğuz, *Mat.–wiss. und Werkstofftech* 32 (2001) 249-252.
40. A. Bayram, A.Uğuz and M. Ula, *Materials Characterization* 43 (1999) 259-269.